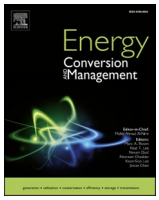
Energy Conversion and Management 332 (2025) 119738



Contents lists available at ScienceDirect

Energy Conversion and Management

journal homepage: www.elsevier.com/locate/enconman



Research Paper



Floating solar wireless power transfer system for electric ships: Design and laboratory tests

Khalifa Aliyu Ibrahim [a], Timothé Le Maréchal [a], Patrick Luk [a], Qing Qin [a], Luofeng Huang [a,*], Ying Xie [b], Patrick Verdin [a], Zhenhua Luo [a]

[a] Faculty of Engineering and Applied Sciences, Cranfield University, Cranfield MK430AL, UK
[b] Faculty of Business and Management, Cranfield University, Cranfield MK430AL, UK

ARTICLE INFO

Keywords:
Floating solar
Wireless power transfer
Maritime decarbonisation
Automate docking system
Wave tank experiments
Electric ships charging

ABSTRACT

The maritime industry is under increasing pressure to decarbonise, presenting an important pathway of transforming the power systems from conventional marine fuels to electric-based. This study proposes an innovative solution to support maritime decarbonisation through the integration of a floating solar clean energy harnessing and wireless power transfer (WPT) technology for electric vessels. The paper presents the design and experimental tests of the integrated system specifically, based on a model of an electric yacht. This study provides an in-depth analysis of application of floating solar to provides an off-grid wireless power transfer system that can scale for larger vessels such as ferries. The off-grid modularity proposed enables scalable, flexible, and sustainable energy delivery for maritime applications and decarbonisation with specific attention to challenges in WPT alignment and environmental condition. Simulations using ANSYS Maxwell were performed to model the magnetic field interactions and ascertain the optimal power transfer efficiency. Subsequently, a reduced-scale prototype system was designed, built and tested in a wave tank. The experimental results demonstrated efficient wireless charging with an average efficiency of 82 %, and the docking system proved effective in maintaining alignment even when the ship has wave-induced motions. The findings support the feasibility of using floating solar WPT systems for maritime vessels and pave the way to larger-scale studies.

1. Introduction

The global maritime industry is one of the largest contributors to greenhouse gas (GHG) emissions, primarily due to its reliance on fossil fuels for propulsion [1]. As the world shifts towards sustainable energy solutions, the decarbonisation of maritime transport has become a pressing priority to reduce greenhouse gas emissions [2]. Electric propulsion for vessels, including yachts and larger vessels like ferries, is seen as a promising solution [3]. By replacing conventional combustion engines with electric motors powered by renewable energy, the maritime sector can significantly reduce its environmental impact. However, the widespread adoption of electric vessels faces several critical challenges, especially in terms of charging infrastructure, which must be efficient, safe, and adaptable to the dynamic conditions at sea. The successful expansion of electric fleets depends on the availability of efficient, zero-emission charging systems, which can operate independently of the existing port grid, given capacity constraints [4,5]. The infrastructure required to support the charging of fully electric vessels is still lacking. Traditional plug-in charging systems are susceptible to environmental degradation, such as corrosion and physical wear, and pose operational challenges in maritime settings where alignment and safety are crucial.

Wireless Power Transfer (WPT) technology offers a potential solution to the charging challenges faced by electric vessels. Unlike traditional charging systems that require physical connections, WPT allows for energy transfer without direct contact between the power source and the vessel. This eliminates the risks associated with electrical connectors in marine environments, such as corrosion, wear and tear, and safety hazards. The WPT technology provides a potential solution to this challenge by enabling contactless, automated charging that can withstand harsh maritime conditions [6]. Moreover, WPT systems can be fully automated, allowing for seamless, hands-free charging processes [7]. The technology is particularly advantageous for vessels that operate in ports or marinas, where docking and charging occur frequently [8].

* Corresponding author.
E-mail address: luofeng.huang@cranfield.ac.uk (L. Huang).

https://doi.org/10.1016/j.enconman.2025.119738
Received 3 December 2024; Received in revised form 3 March 2025; Accepted 10 March 2025
0196-8904/© 2025 The Author(s). Published by Elsevier Ltd. This is an open access article under the CC BY license (http://creativecommons.org/licenses/by/4.0/).

Additionally, the integration of renewable energy sources into the charging infrastructure is essential to achieving true decarbonisation in maritime transport [9]. Karimi et al. [10]conducted review of shore-to-ship charging systems including wired, wireless, and battery swapping solutions, focusing on the power system architecture and control strategies for efficient charging. Their research focuses on shore-based charging infrastructure for battery-powered ships, emphasizing power system architecture and control mechanisms in port environments. In addition, challenges in shore-based power systems and their dependency on grid availability was also discussed. Mahdi et al. [11]provide a comprehensive review of shore-to-ship and shipboard power converters, highlighting advancements in conductive connections, frequency converters, and semiconductor technologies such as SiC and GaN. Their work focuses primarily on the grid-connected architectures for large ships and the potential for modular converters in high-power applications. Rong et al. [12] investigate a capacitive power transfer (CPT) technology, particularly the design and optimization of a five-plate coupler, achieving high efficiency in high-power applications. While their work offers valuable insights into the efficiency and performance of CPT systems, their work did not experiment with the docking process or the charging arm of WPT for maritime applications. The laboratory test did not include the charging process of the boat, which has its unique characteristics. Therefore, there is a need for a sustainable, off-grid wireless power transfer (WPT) solution that eliminates reliance on shore-based charging infrastructure, particularly for remote maritime operations. By addressing these challenges employing floating solar systems, it would contribute to the advancement of autonomous, and sustainable maritime electrification.

A floating solar power plant consists of individual photovoltaic (PV) panels, with which the scale is flexible as the total panel number can be fine-tuned according to the power requirement. The modular design makes floating solar farms easy to install and flexible in shape and location, with high applicability to the water space inside and outside the harbour of a port [13]. A key challenge in supporting the electrification of maritime vessels is the limited capacity of existing electrical grids at ports [14], which are often unable to handle the high-power demands of charging multiple electric vessels simultaneously. To address this, the integration of floating solar power plants presents a promising alternative [15]. Floating Solar (FS) systems provide renewable energy directly at the point of use, thereby reducing the reliance on the grid and overcoming existing capacity limitations. The deployment of floating solar panels on water surfaces, such as port basins, offers an efficient way to harness renewable energy while making optimal use of available space. By combining floating solar with WPT systems, ports can create a self-sustaining charging infrastructure for electric yachts and ferries. It can significantly contribute to the decarbonisation of the maritime sector and ensuring a reliable energy supply without placing additional strain on the grid. While some progress has been made in developing WPT technologies for smaller vehicles like electric cars, the maritime environment introduces additional complexities. Furthermore, the lack of a robust and adaptable docking system further limits the practicality of WPT systems for yachts and larger vessels.

In WPT systems, maritime applications however, introduce additional complexities such as wave-induced motion, tidal variations, and unpredictable weather conditions [16]. While WPT for small-scale vessels has promising results, there is limited research on systems developed and the challenge of alignment in dynamic maritime environments have not addressed. Moreover, there is an urgent need in research on integrating WPT systems with renewable energy sources, such as floating solar farms, which could provide a self-sustaining solution for charging electric vessels. The integration of a robust docking mechanism that can ensure precise alignment between the transmitter and receiver is key to overcoming the limitations of existing systems. This paper seeks to address these gaps by introducing a novel floating solar WPT (FSWPT) docking system tailored for electric yachts charging. This paper aims to design, simulate, and experimentally evaluate a WPT system specifically for yachts and exploring its potential scalability for larger vessels. We design of a small-scale prototype with a novel mechanical alignment mechanism to maintain efficient charging is subjected to induce waves to assess the performance of the system. ANSYS simulations were conducted to evaluate the magnetic field and coupling coefficient between the transmitter and receiver coils to identify the optimal conditions for maximum power transfer. A complete 50 W prototype FSWPT system was developed and tested experimentally to demonstrate the functionality of the system in a wave tank as shown in Fig. 1. This paper presents several key contributions to the field of maritime electrification and WPT technology for maritime applications.

I. The design and implementation of a floating solar-powered WPT system providing a scalable and flexible solution for maritime charging infrastructure.
II. Proposed a grid independent system approach based on floating solar charging for the wireless charging system as a path for maritime decarbonisation applications.
III. Introduce a novel docking mechanism that includes an automatic gate, designed to address the misalignment challenges faced during wireless charging of yachts in dynamic maritime conditions.
IV. Design a novel robot arm that improve transmitter and receiver alignment to enhance power transfer in maritime harsh environments.
V. We experimentally validate the system's effectiveness simulating real-world conditions using a wave tank, providing valuable insights on how the FSWPT can be applied not only to yachts but also applicable to vessels or ferries.

The rest of the paper is organized as follows; Section 2 provides a detailed description of the methodology, including the design of the docking system, the simulation setup using ANSYS Maxwell, and the experimental procedures. Section 3 presents the results of the simulations and wave tank experiments, focusing on power transfer efficiency and system alignment. Section 4 offers a discussion of the results, highlighting the system's potential scalability for larger vessels such as ferries and addressing the key challenges and limitations identified during the study. Finally, Section 5 concludes the paper by summarizing the key findings and proposing future research directions, particularly in optimizing the docking system for open-water applications and integrating renewable energy sources into the maritime WPT infrastructure.

2. Methodology

An iterative design methodology that incorporated simulations and prototyping was adopted in this project. The methodology consists of designing the docking and alignment system, simulation of power transfer efficiency, and experimental testing of the system prototype in a wave tank.

2.1. Yacht and docking system design

In this study, we modified a high-performance, ready-to-run Yacht model from Heng Long Salina RC Speed Boat and tested it in the WPT system. The modifications allow the Yacht include fitting the WPT receiver, battery with its management system, and other electronic components to enable alignment and efficient power transfer under simulated maritime conditions, thereby expanding its application towards experimental research in sustainable marine power solutions. The Yacht model with 705 mm length, a beam of 195 mm and a height of 310 mm originally designed for speed and manoeuvrability in controlled water environments which makes it suitable for this research. The electric boat can reach a maximum speed of 30 km/h, powered by a 2000 mAh, 8.4 V Ni-MH rechargeable battery, providing a runtime of 10–15 min with a range of up to 250. Fitted with dual high-performance

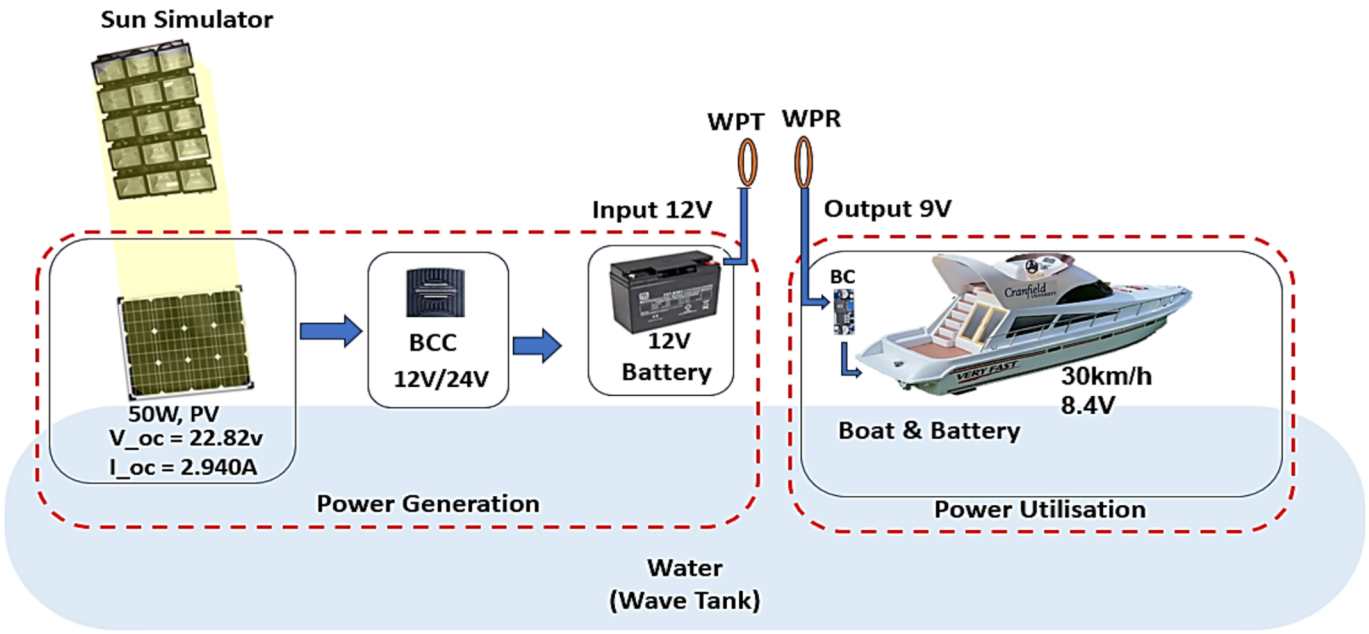


Fig. 1. FSWPT 50 W system block diagram.

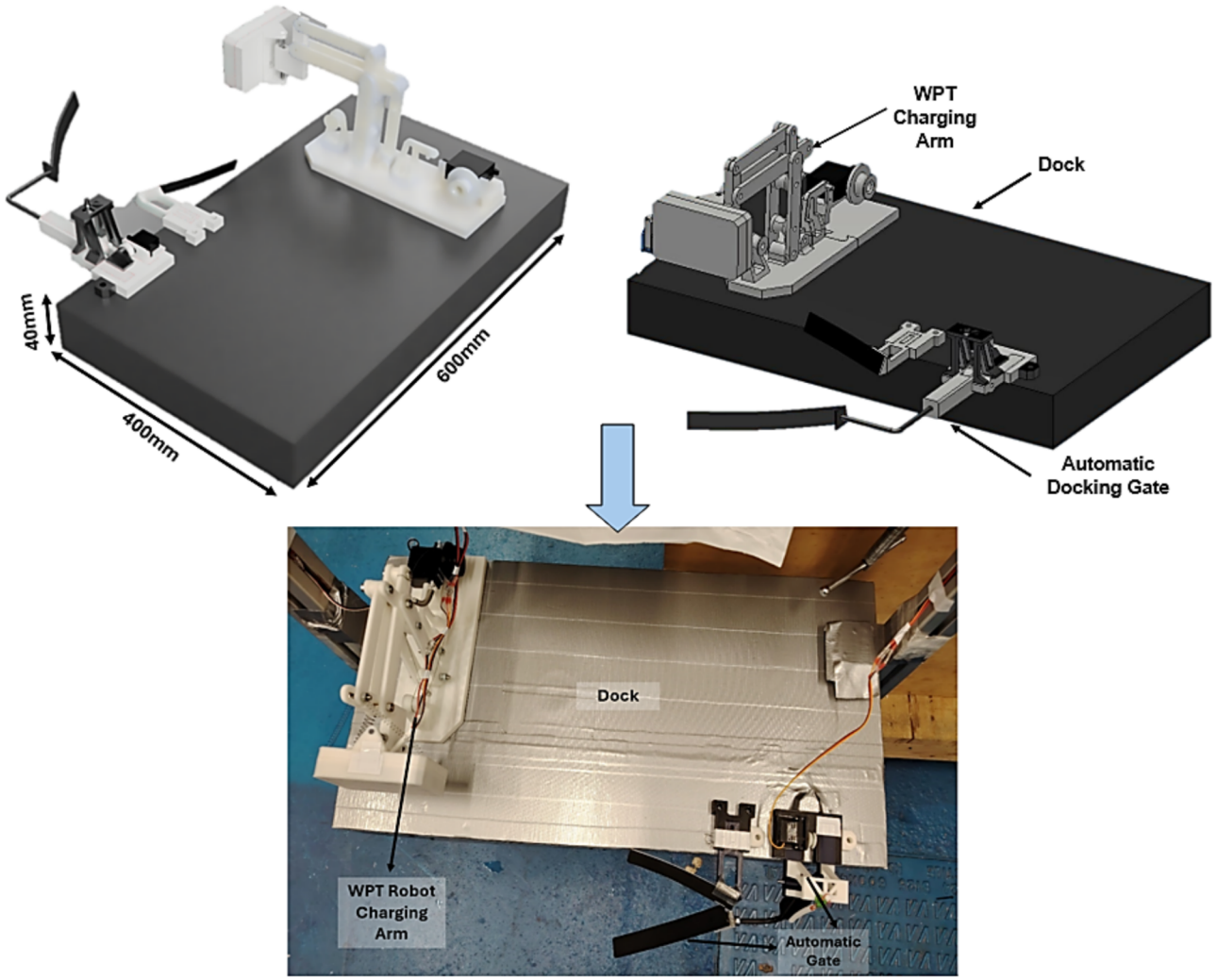


Fig. 2. Docking system design CAD model and prototype.

motors for enhanced power and controlled with 2.4 GHz radio transmitter includes a waterproof compartment for added durability. The WPT receiver was integrated with the boat to allow wireless charging when docked in the docking system proposed in Fig. 2.

The successful implementation of a WPT system in maritime environments requires precise alignment between the transmitter onshore and the receiver onboard the yacht. To address this challenge, a docking system was designed, incorporating an automatic gate and a novel robotic arm with a transmitter holder to ensure precise alignment during charging. The automatic gate is a key feature of the docking system, providing a secure method for guiding the yacht into the correct position for charging. This system minimizes the risk of misalignment between the WPT transmitter and receiver, which can drastically reduce charging efficiency. Fig. 2 shows the CAD model and the fabricated docking system design. The dock is made up of polystyrene with 40 mm thickness, 400 mm width, and 600 mm length which the WPT charging arm robot and automatic gate is mounted on. The floating solar, WPT system, charging arm, and dock were assembled on a wave water tank to demonstrate the WPT alignment charging and docking process. A small scaled 50 W charging system procedure is designed and demonstrated. This reduced-scale system allows to test the core principles of wireless power transfer (WPT) in a controlled environment before scaling up to larger systems. Although the power transfer is limited to 50 W, it serves as a critical starting point for understanding the behaviour of WPT systems in dynamic maritime conditions. The circuit and mechanical designs are appropriately scaled to match the experimental setup and the specifications of the small-scale boat, which is designed to operate in the lab's wave tank. The mechanical alignment mechanism as shown in Fig. 2 was designed in Autodesk Fusion 360. The components were 3D printed using a CREALITY 3D printer. The 3D printing process allowed for rapid prototyping and iteration, ensuring that each component was optimised for strength, precision, and durability.

A key challenge in WPT systems for maritime environments is the alignment of the transmitter and receiver, particularly in the presence of wave-induced motion as reported in [17]. To solve this, a three degree of freedom (3-DOF) robotic arm fitted with tension springs was developed to hold and position the WPT transmitter. The robotic arm was designed to dynamically adjust its position in response to waves mechanically using springs, ensuring that the transmitter remains aligned with the receiver throughout the charging process. The transmitter holder is fitted to the arm and can move in four direction enabling real-time adjustments that compensate for minor shifts in the yacht's position due to environmental conditions. The fitted spring absorbs any minor impacts or shifts caused by wave motion, ensuring that the receiver remains aligned with the transmitter throughout the charging process. The server motor enables WPT engagement, and disengagement of the charging process. The complete video of the docking and charging process can be found in the supplementary section. The WPT transmitter and receiver CAD model skitch and prototype are shown in Fig. 3. The transmitter coupling charging mechanism was fitted with four 10 mm diameter N52 magnets which are transitioned using the servo motor to align with the magnets at the receiver during the charging process. The receiver holder was designed, 3D printed and fitted on the boat for use in the experimental prototype. The WPT specification is presented in Table 1.

The series-series (SS) WPT topology is adopted due to its suitability for high frequency wireless power transfer as reported in [18] and [19]. A typical series-series compensated WPT system is shown in Fig. 4. The capacitors C_1, C_2 and inductance L_1, L_2 are used to tune the circuits to their resonant frequencies, maximizing power transfer efficiency. The mutual inductance M indicates the degree of coupling between the transmitting and receiving coils. In the equivalent circuit diagram, V_s represents the source voltage where $j\omega$ term represent the complex

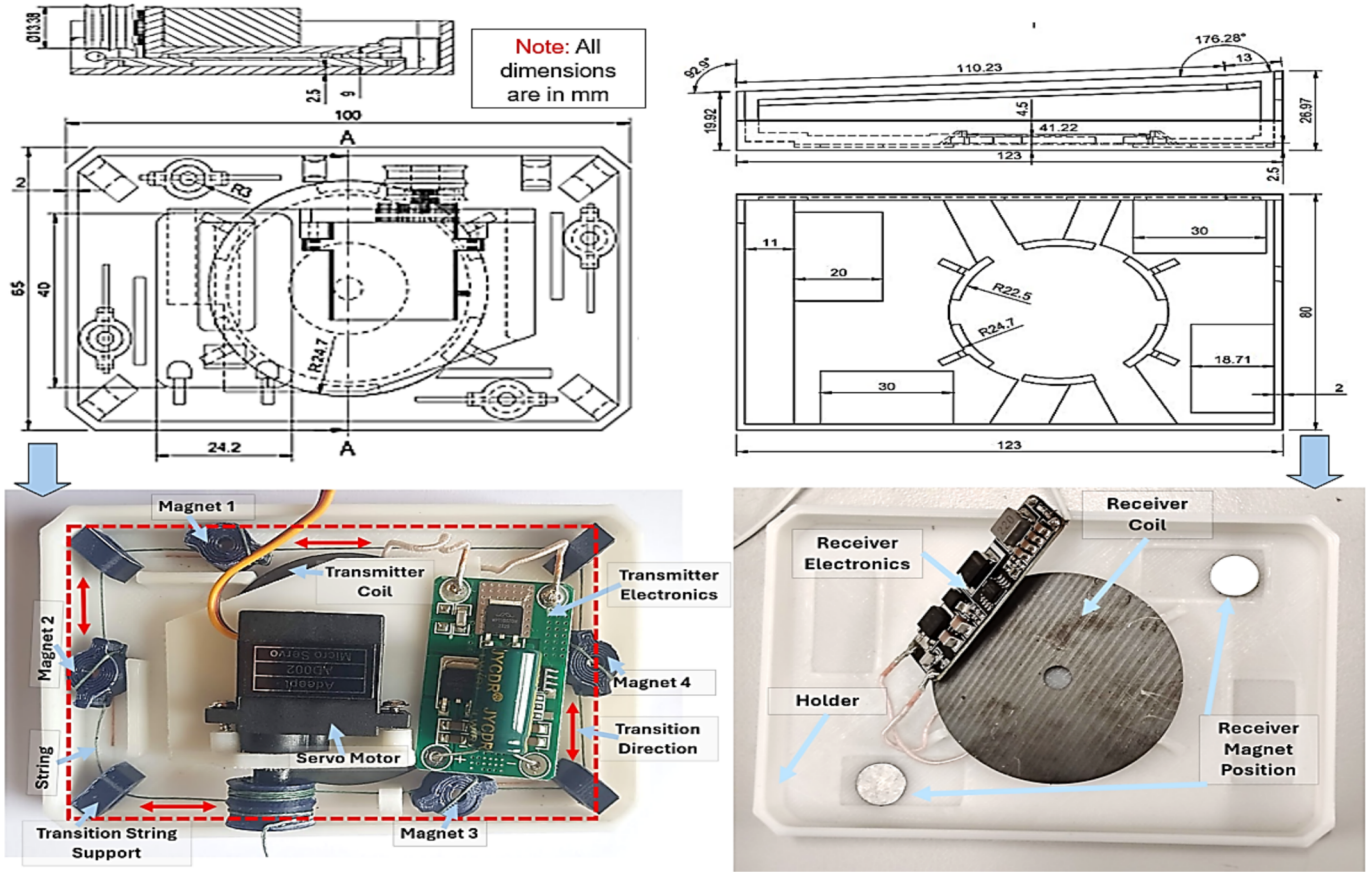


Fig. 3. WPT transmitter and receiver CAD model sketch and prototype developed.

Table 1
WPT specifications.

Parameter (Unit)	Value
Switching frequency (kHz)	85
Diameter of Coil (mm)	50
Diameter of Hole Inside (mm)	5
Thickness of Coil (mm)	3.5
Diameter of Wire (mm)	1.2
Litz Wire	0.08 mm × 105 Strands
Self-Inductance (μH)	24
Quality Factor	20
Number of Turns	20
Resistance (Ω)	0.0467
Capacitance (μF)	27.55
Magnetic Shielding Thickness (mm)	0.6

impedance of the components in the primary and secondary side as given by Equations (1) and (2). Equation to represent the boat side.

$$V_s = (R_1 + R_s + j\omega L_1 + \frac{1}{j\omega C_1})I_1 + j\omega M I_2 \tag{1}$$

$$0 = (R_L + R_2 + j\omega L_2 + \frac{1}{j\omega C_2})I_2 + j\omega M I_1 \tag{2}$$

Where R_s represent the resistance of the source and R_1 correspond to the resistances in the primary circuit, R_2 represents the resistance in the secondary circuit and R_L models the boat battery as electrical load connected to the receiver. The currents I_1 and I_2 represent the current flowing through the primary and secondary circuits, respectively. At resonance frequency, the capacitive reactance cancels out the inductive reactance. Thus, the resonance condition is given by Equations (3) and (4) resulting in reduced power losses.

$$V_s = (R_1 + R_s)I_1 + j\omega M I_2 \tag{3}$$

$$0 = (R_L + R_2)I_2 + j\omega M I_1 \tag{4}$$

The total impedance of the primary circuit Z_1 and secondary circuit Z_2 considering the resistances, inductance, and capacitance is given by Equations (5) and (6).

$$Z_1 = R_1 + R_s + j\omega L_1 + \frac{1}{j\omega C_1} \tag{5}$$

$$Z_2 = R_L + R_2 + j\omega L_2 + \frac{1}{j\omega C_2} \tag{6}$$

Substituting Equations (5) and (6) into Equations (1) and (2) gives Equation (7) and (8) and solving for I_1 and I_2 through Equations (9), (10), and (11) gives Equations (12) and (13). The input power of the wireless power transfer transmitter at the docking side is given Equation (14) and Equation (15) represent the input power at the boat side.

$$V_s = Z_1 I_1 + j\omega M I_2 \tag{7}$$

$$0 = Z_2 I_2 + j\omega M I_1 \tag{8}$$

$$I_2 = -\frac{j\omega M I_1}{Z_2} \tag{9}$$

$$V_s = Z_1 I_1 + \frac{j\omega M(-j\omega M I_1)}{Z_2} \tag{10}$$

$$V_s = I_1\left(Z_1 + \frac{\omega^2 M^2}{Z_2}\right) \tag{11}$$

$$I_1 = \frac{V_s Z_2}{Z_1 Z_2 + \omega^2 M^2} \tag{12}$$

$$I_2 = -\frac{j\omega M V_s}{Z_1 Z_2 + \omega^2 M^2} \tag{13}$$

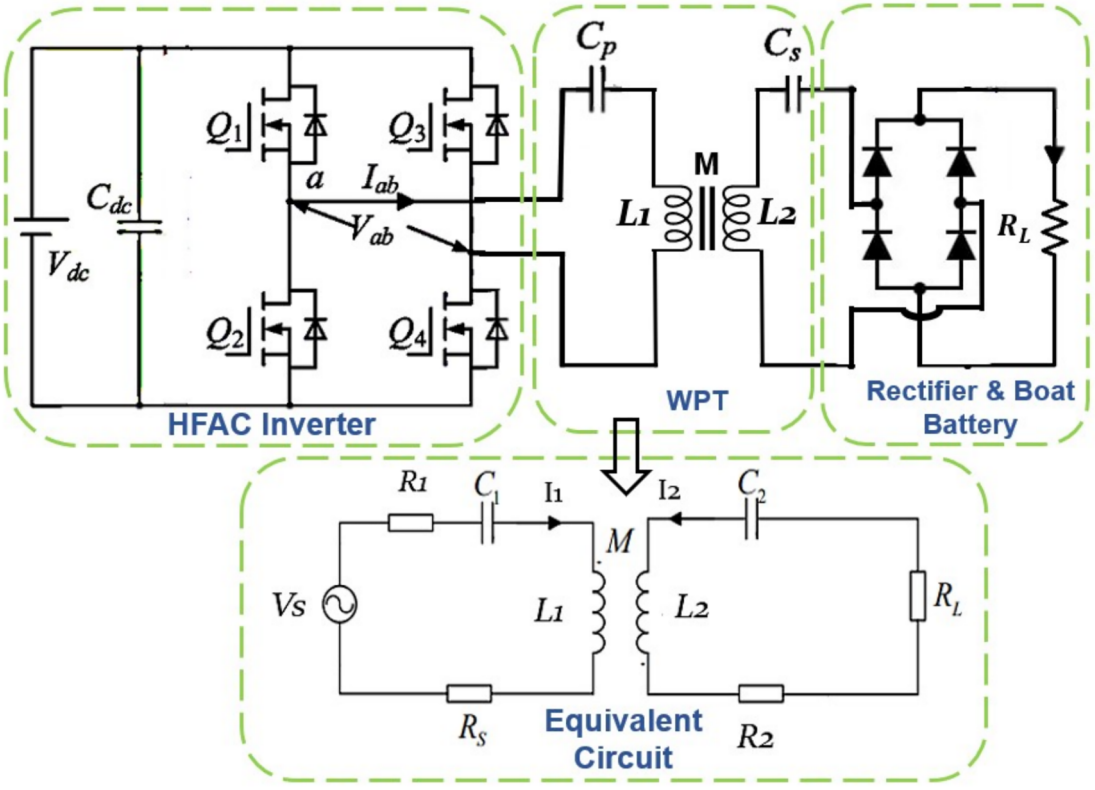


Fig. 4. WPT with series-series resonance compensation network and equivalent circuit.

$$P_{input_docking} = V_s I_1 = V_s\left(\frac{V_s Z_2}{Z_1 Z_2 + \omega^2 M^2}\right) \tag{14}$$

$$P_{out_boat} = I_2^2 R_L = \frac{(\omega M V_s)^2 R_L}{Z_2(Z_1 Z_2 + \omega^2 M^2)} \tag{15}$$

Equation (16) can be used to calculate the resonant frequency (f_o) as a function of inductance and capacitance. A WPT coil inductance depends on the number of turns (N), coil circular radius (R), the permeability of empty space (μ_o), the relative permeability (μ_r), and the G.M.R of the wire (r) as shown in equations (17).

$$f = \frac{1}{2\pi\sqrt{LC}} \tag{16}$$

$$L_o = N_o^2 R \mu_o \mu_r [ln\left(\frac{8R}{r}\right) - 2] \tag{17}$$

Where L_o represent the self-inductance of the coils for load matching between transmitter and receiver. The primary capacitance can be calculated considering the secondary inductance, secondary capacitance, and primary inductance as shown in equation (18). The coupling coefficient (k) is given by equation (19) ranges from $0 \leq k \leq 0.5$ for a loss coupling [18]. These provide an estimate of the degree of magnetic coupling existing between two inductors where (M) is the mutual inductance. The quality factor (Q) is given by equation (20) which can be used to measure the efficiency of the resonant circuit as a ratio of inductive reactance to resistance on the primary and secondary sides where $\omega = 2\pi f$. Maximum efficiency can be calculated using equation (21) considering the coupling coefficient and quality factors of the primary and secondary sides, or currents through the primary and secondary sides with load resistance, primary and secondary resistances as shown in equation (22). The optimum efficiency can also be calculated using equation (23), where U is the merit figure that needs to be maximal for a better efficiency and Q_1 and Q_2 are primary and secondary quality factors. These equations provide the basis of designing optimised WPT.

$$C_1 = \frac{L_2 C_2}{L_1} \tag{18}$$

$$k = \frac{M}{\sqrt{L_1 C_2}} \tag{19}$$

$$Q = \begin{cases} \dfrac{\omega L_1}{R_1}, ForPrimarySide \\ \dfrac{\omega L_2}{R_2}, ForSecondarySide \end{cases} \tag{20}$$

$$\eta = \frac{k^2 Q_1 Q_2}{(1 + \sqrt{1 + k^2 Q_1 Q_2})^2} \tag{21}$$

$$\eta = \frac{I_2^2 R_L}{I_1^2 R_1 + I_2^2 R_2 + I_2^2 R_L} \tag{22}$$

$$\eta_{opt} = \frac{U^2}{1 + \sqrt{1 + U^2}}, \text{ where } U^2 = k\sqrt{Q_1 Q_2} \tag{23}$$

The schematic diagram presented in Fig. 5 illustrates the control circuit of a docking and WPT system, using a microcontroller to manage multiple servo motors. The circuit is configured with three servo motors (J_1, J_2, and J_3) that are connected to the digital output pins of the controller, allowing for precise actuation control. J_1 is associated with the WPT indicated in Fig. 4, J2 is associated with the robotic movement of the WPT arm based on Fig. 3, and J3 is associated with the automatic gate based on Fig. 2. Each servo motor receives a pulse signal and is powered by a 5 V supply. Additionally, two push-button switches (S_1 and S_2) are included in the circuit, interfaced with pull-down resistors (R_1 and R_2, each 220 Ω) to ensure accurate state readings, preventing floating inputs. These switches provide manual control inputs to the controller for initiating specific docking actions. Furthermore, the circuit incorporates two LEDs indicators (LED_1 and LED_2), each emitting red light, which serves as visual indicators for docking status or system alerts. These LEDs are connected in series with current-limiting resistors

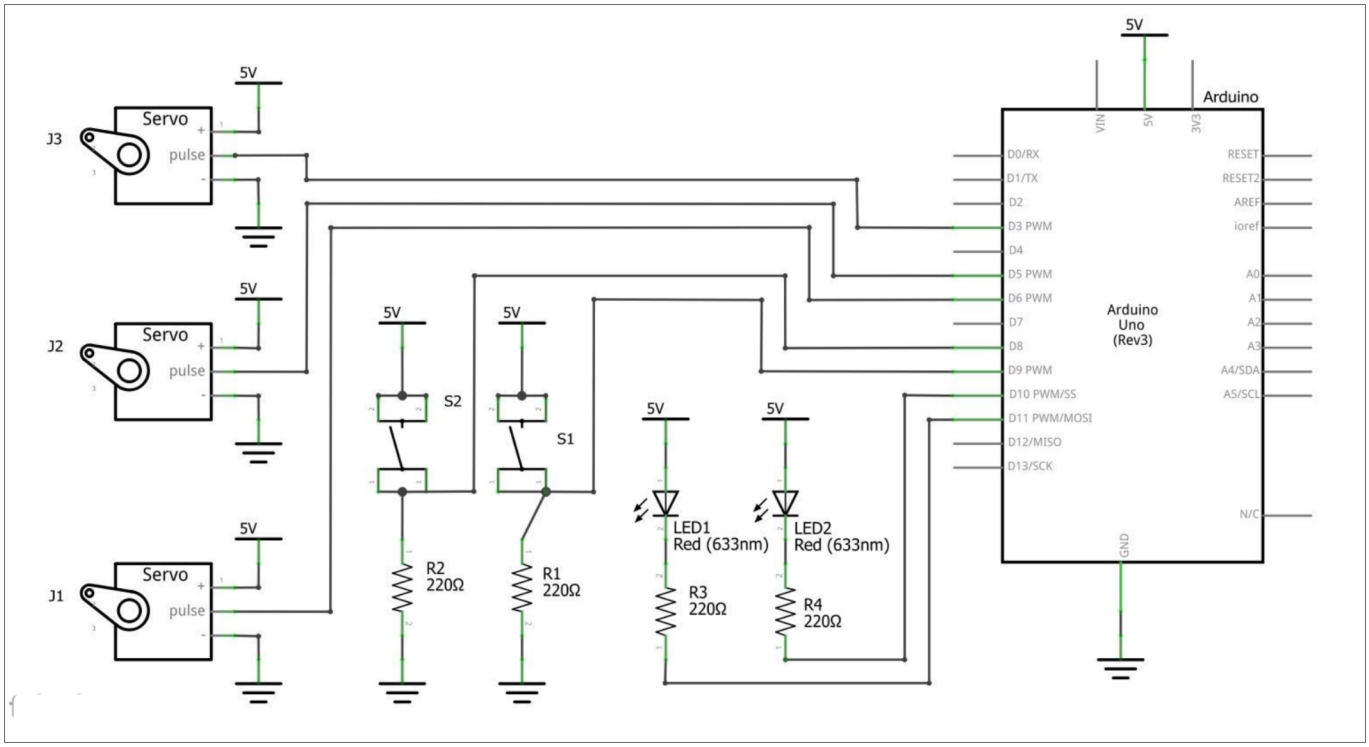


Fig. 5. Simplified automatic gate, docking and WPT system control circuit schematic diagram.

(R_3 and R_4, each 220 Ω) to protect them from excessive current. The LEDs are controlled via digital output pins of the controller, which allows them to illuminate based on the system state, providing feedback to the user. The entire system operates on a 5 V power supply, which is distributed to the components appropriately.

This control circuit effectively integrates servo motors, user input switches, and visual indicators to create a robust docking system, demonstrating the integration of mechanical actuation and feedback control through a microcontroller-based architecture. The power system circuit schematic shown in Fig. 6 represents the FSWPT which integrates components for efficient power conversion, storage, and management. The power generation section of the system is the FSS connected to a KLD solar charge controller (Mod1), which regulates the charging process and ensures safe charging of the 12 V. The solar charge controller has distinct connections for the solar panel, battery, and load, effectively controlling the power distribution based on the availability of solar energy and the battery's state of charge. The 12 V battery serves as the primary energy storage unit, supplying power to an inverter (M_2), which converts direct current (DC) from the battery into high frequency alternating current (HFAC) for the WPT transmitter (L_1) and receiver (L_2). The receiver output is then fed to a rectifier (M_3)fitted with a blue LED indicator that converts the AC back to DC, which is connected to a boost converter component within the boat system battery management. The boost converter (XL6009E1) is employed to further increase the voltage as required for specific downstream components, optimizing energy utilization and providing appropriate power levels. The system also includes a battery charging level indicator (LED_1), connected via a current-limiting resistor (R_1, 10kΩ), which functions as a visual indicator of the operational status of the boat battery. The motor (M_4) driving the boat is powered by an 8.4 V. A diode (D_1, 1 N4001) is included to prevent reverse current flow, thereby protecting the components from potential damage.

The power system circuit provides a comprehensive solution for energy conversion, storage, and distribution, effectively integrating renewable energy sources and maintaining operational stability through careful voltage and current management. The complete specifications of the simplified FSWPT power circuit system and control circuit are presented in Table 2.

2.2. ANSYS simulations

The simulations conducted using 2024R2 ANSYS Maxwell provided valuable insights into the magnetic field interactions between the WPT transmitter and receiver with the magnetic coupling transitioning design discussed in Fig. 3. In addition, it provides sensitivity to misalignment as well as ensures that no magnetic field interference. The WPT system was modelled as a series of transmitter and receiver coils designed to operate at a frequency of 85 kHz. In addition, the simulation aimed to evaluate the magnetic coupling between the transmitter and receiver coils and to identify the optimal alignment conditions for maximum power transfer. Key parameters included the distance between the transmitter and receiver, the degree of misalignment, and the strength of the magnetic field. The simulation results provided insights into the effects of misalignment on power transfer efficiency, helping to optimise the design of the docking system and alignment mechanisms. Fig. 7 shows the coil simulation including the magnetic shielding. The results showed that the magnetic field was well-contained within the transmitter,

Table 2
Complete system specifications.

Schematic	Label	Part Type
FSWPT System Circuit Design	Battery 12 V, LIPO-2000 mAh	Floating Solar Energy Storage
	8.4 V, 1000 mAh	Boat Battery
	3.0–30 V	Boost Converter
	D1	Diode
	L1, L2	Litz Wire of Transmitter Coil, Receiver Coil
	<10 mA, 5–30 V DC	Charging indicator
	M4	DC Motor (Boat Drive)
	Mod1	KLD Solar Charge Controller
	Part1	Floating Solar Panel, 50 W
	R1	10kΩ Resistor
Control Design	Microcontroller	Arduino Uno (Rev3)
	AD002 Basic Servo	J1, J2, J3
	LED1, LED2	Red LED – 5 mm
	R1, R2, R3, R4	220 Ω Resistor
	S1, S2	Pushbutton

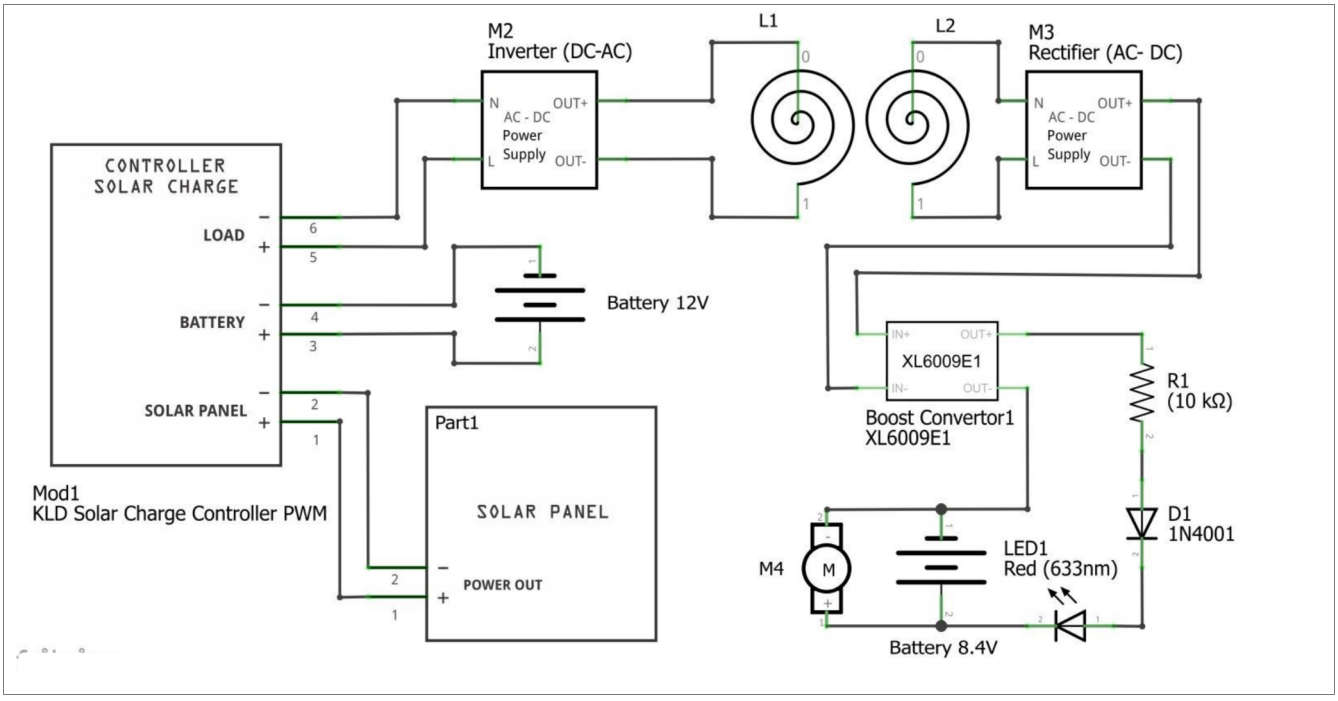


Fig. 6. FSWPT simplified power circuit system schematic diagram.

minimizing the risk of electromagnetic interference (EMI) with other onboard components as shown in the simulation video provided in the supplementary material. This containment is essential for maintaining safety and functionality in real-world maritime environments, where multiple electronic systems operate in proximity. The coupling coefficient k must be determined by simulation.

The simulation of the magnetic field is presented in Fig. 8. The heat map (Fig. 8a) of the magnetic field intensity during power transfer. It can be observed that the magnetic field remains contained between the two ferrite shields, ensuring that these transmitters and receivers can be used safely in the prototype. The ferrite shielding is sufficient, and none of the other devices in the vicinity of the WPT will be affected by this magnetic field. This information is useful for the design of the prototype, as it allows other components to be placed within a few centimetres of the WPT without interference. To assess the optimal working range between the transmitter and the receiver in terms of the efficiency for the WPT, the coupling coefficient k was calculated for distances between. The curve representing the value of k as a function of distance is shown in Fig. 8(b). The value of the coupling coefficient decreases as the distance increases. From the value of k, the simulated optimal efficiency is determined using equation (8) to compare with the experiment efficiency, which will be presented in Fig. 11(d).

2.3. Assembly and experimental setup

The complete system prototype was assembled and tested in a wave tank at Cranfield University. The WPT experiment was conducted with calm water and under different wave amplitudes (A) from 0.001 m to 0.010 m at an interval of 0.002 m with a frequency of 0.5 Hz and run time of 90 s in a wave tank. The wave tank has a width of 1.5 m, a height of 2 m, and a water depth of 1.9 m that contains a wavemaker which mimics coastal wave activities based on the ship model [20]. The primary goals of the experiment were to assess WPT efficiency based on the magnetic coupling mechanism proposed in Fig. 3, and the docking system stability to wave as well as evaluate the performance of the automatic gate and robotic arm in maintaining alignment during wave-induced motion. A video showing the WPT with an induced wave can be found in the supplementary section. During the experiment, real-time data on power transfer efficiency, alignment accuracy, and system stability were collected. The robotic arm's ability to adjust the transmitter's position dynamically was monitored, and the power transfer efficiency was measured continuously throughout the charging process. Data from the proximity sensors on the automatic gate and robotic arm were analysed to assess how well the system maintained alignment in challenging conditions. Fig. 9 presents the experimental setup with a floating solar panel integrated with an electric boat in a controlled wave tank environment. This allows the study of the floating solar charging system performance in varying scenarios. A sun simulator, providing a light intensity of approximately 1000 lm, is positioned above the setup to emulate sunlight, facilitating realistic testing conditions for the floating solar panel and its integration with the electric boat system.

Fig. 10 depicts the docking system experimental setup, designed to assess the interaction between the electric boat and the docking mechanism. The setup includes a floating solar panel, which supplies energy to the system, and a water tank to simulate realistic conditions. The electric boat features a battery level indicator to monitor its power status, ensuring that the boat docks appropriately when recharging is necessary. Motion sensors are employed to detect the boat's approach, and a coupling arm guides the boat into the docking position. The dock includes an automatic gate that manages the boat's entry and exit. This setup provides a comprehensive platform for studying the docking process, power transfer efficiency, and the coordination between the boat and docking components, thereby validating the system's functionality under controlled experimental conditions.

The wave performance data collected on the boat and WPT coupling arm were obtained using two wave motion sensors. The sensor recorded acceleration, angular position, and angular velocity data in the X, Y, and Z directions on the WPT coupling arm and another for the boat, providing a comprehensive dataset for analysing the system's behaviour. The acceleration data were recorded in units of gravity (g) after which the data were processed using Python to determine the corresponding forces acting on the components. The recorded acceleration values were converted from (g) to meters per second squared (m/s^2) with a factor of 9.80665 m/s^2. The forces in the X, Y, and Z directions (F_x, F_y and F_z) were then calculated using Newton's second law of motion $F = ma$. Where a is the acceleration and m is the mass of the boat or WPT robotic charging arm. These calculated forces were then plotted over time to visualize the dynamic effects of wave interactions and to show how the components responded to wave-induced motion on both the boat and the coupling arm. In addition, a plot of angles and angular

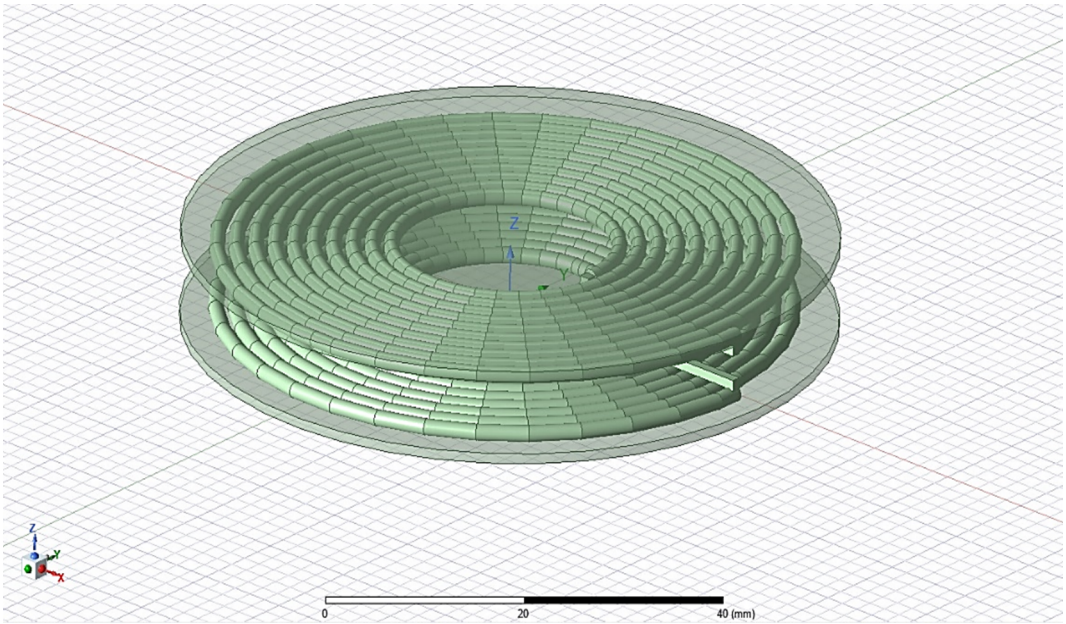


Fig. 7. ANSYS Maxwell interface for electromagnetic interference simulation.

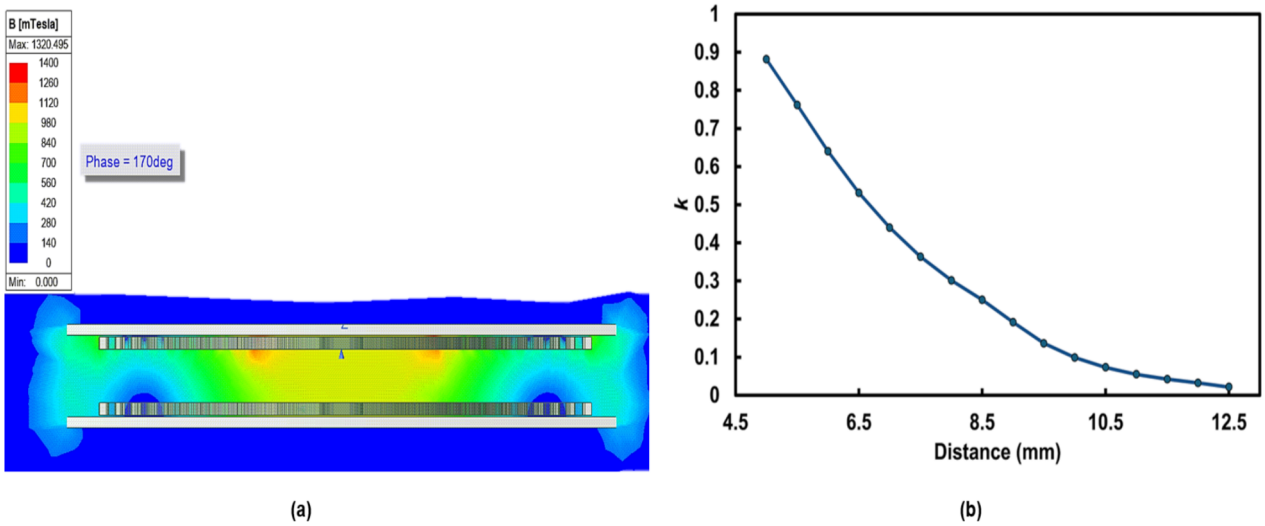


Fig. 8. Electromagnetic field simulation (a) magnetic field intensity (b) power transfer coupling coefficient.

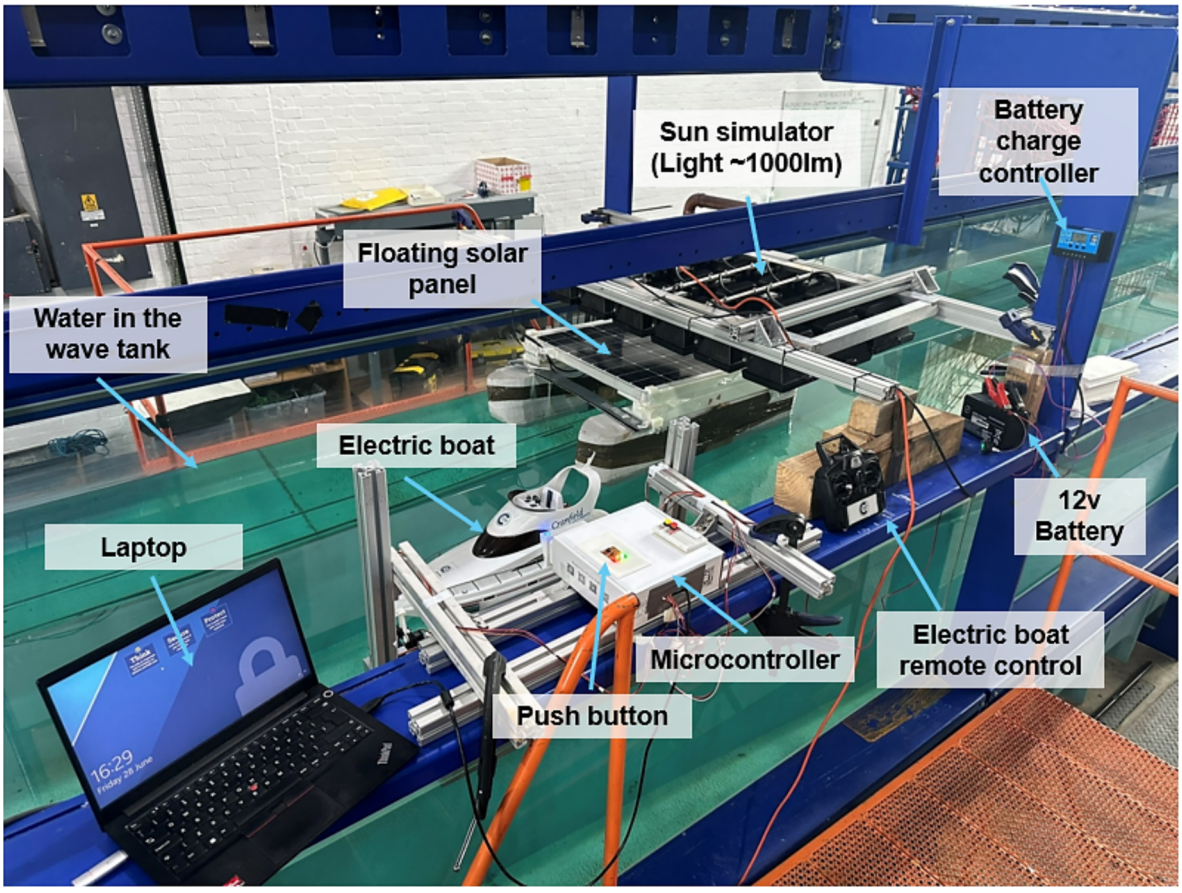


Fig. 9. Overview of the experimental setup.

velocities X, Y, and Z directions over time are also plotted. The angles provided insights into the changes in orientation due to wave disturbances, while the angular velocities captured the rate of change in orientation, highlighting the rotational dynamics. The acceleration data, after conversion, were also plotted to show how the components responded to wave-induced motion. These plots, allowed for a comprehensive analysis of the system's behaviour under varying wave conditions, providing insights into the forces, orientations, and dynamic responses of the FSWPT system. This ensured that the WPT system remained effective under challenging conditions, validating the stability and robustness of the design.

3. Results

This section discusses the performance of the WPT with and without FSP, calm-water tests, and wave tests of the FSWPT system. The calm test considers the performance of the WPT charging mechanism, and the wave test considers simulated marine environmental conduction with

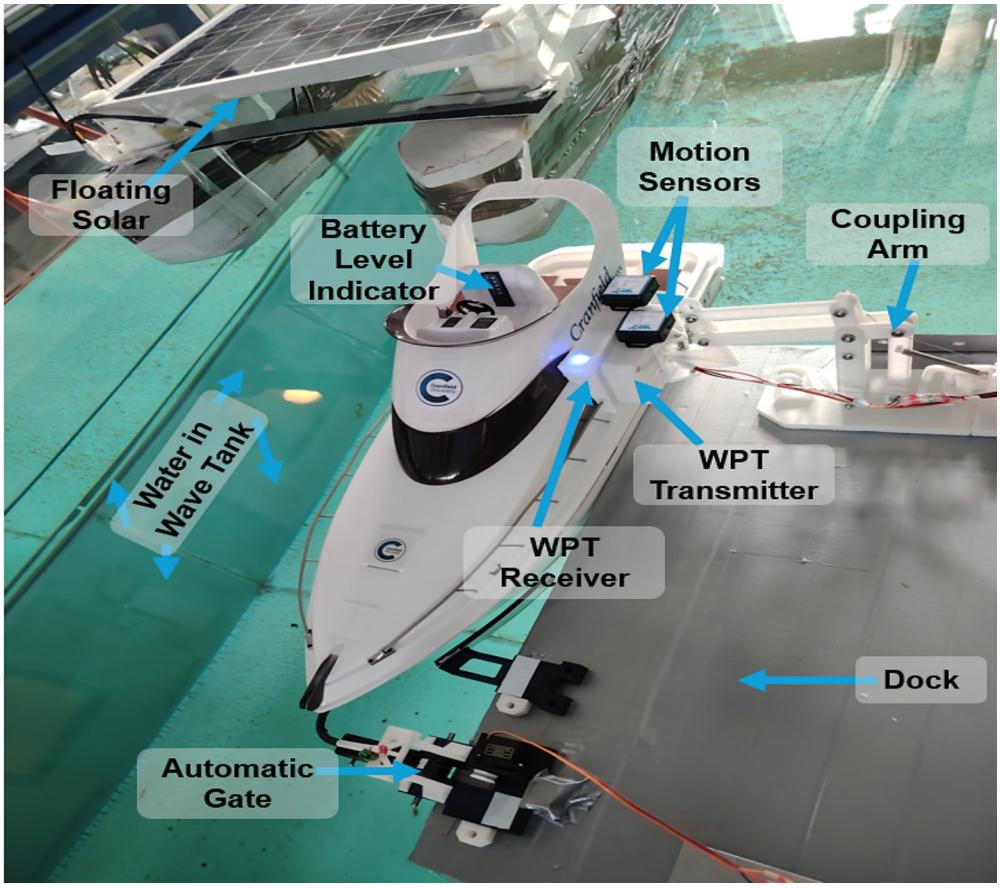


Fig. 10. Docking system setup.

induced waves.

3.1. Calm-Water tests

Fig. 11 (a) to (d) shows the WPT experimental test performance between the transmitter and receiver over different distances. In Figure (a), the variation of input and output voltage and current with respect to distance is depicted. The result show that while the voltage remains stable, the current decreases as the distance between the transmitter and receiver increases. This indicates a reduction in power transfer efficiency as separation grows. Similarly, Figure (b) shows the variation in power input and power output across different distances. It can be observed that power decreases as the distance increases, which is consistent with the expected performance of WPT systems, where efficiency declines at greater distances due to weaker coupling. Figure (c) presents the WPT efficiency of the docking system, comparing the performance of the full system integrated with direct connection to a floating solar (FS) and without the FSP (battery only). The results indicate that the efficiency remains high for both cases up to 9 mm, beyond which a significant drop in efficiency occurs, particularly for the system without the FS. This demonstrates the beneficial impact of the PV energy storage to maintaining efficient charging in the absent of solar irradiance or at night. Figure (d) compares the experimentally measured efficiency with simulated values as a function of distance. The trends for both experiment and simulation are in good agreement, showing a high efficiency up to approximately 8 mm, after which there is a notable decline. The consistency between experimental and simulated results validates the model's accuracy in predicting the system's magnetic field interactions between the WPT transmitter and receiver. These figures demonstrate that the optimal operational range for efficient power transfer is maintained at less than 8–9 mm distance, highlighting the critical role of distance and shielding in the performance of WPT in the docking systems.

Fig. 12 (a) and (b) shows the forces experienced in different components of the docking system during wireless, focusing on the boat and the WPT coupling arm, respectively. In Figure (a), the time series of forces in the X, Y, and Z directions acting on the boat is the actual time when the data is recorded. After the boat dock, it was observed that there are significant variations in forces during different phases of WPT operation, including engagement (E), disengagement (DE), up to the boat leaving the dock (LD) after disengagement. Specifically, the fluctuations indicate transient forces encountered on the boat when the WPT robotic arm on the docking station engages, disengages, and eventually when the boat leaves the dock. The stabilization between E and DE is when the WPT charging is takes place once the boat is securely docked. These force patterns are crucial for ensuring precise positioning and minimizing impact during the docking process. Similarly, Figure (b) represents the forces in the X, Y, and Z directions acting on the WPT coupling arm. The engagement (E), disengagement phase 1 (DE1), and disengagement phase 2 (DE2) are indicated on the plot, showing variations in forces corresponding to these different stages. During DE1, the aligning magnets demagnetize, disrupting the alignment between the WPT receiver and transmitter, leading to notable force changes in the X, Y,Z direction. In DE2, the arm retracts back while the automatic gate opens, allowing the boat to leave the dock, resulting in additional force variations. The stabilization of forces following these peaks is critical for maintaining a stable coupling between the boat and the docking station, ensuring effective WPT. The analysis of these force profiles provides insight into the dynamic interactions between the boat and coupling arm, highlighting areas that may require further design optimization to achieve smoother engagement and docking stability.

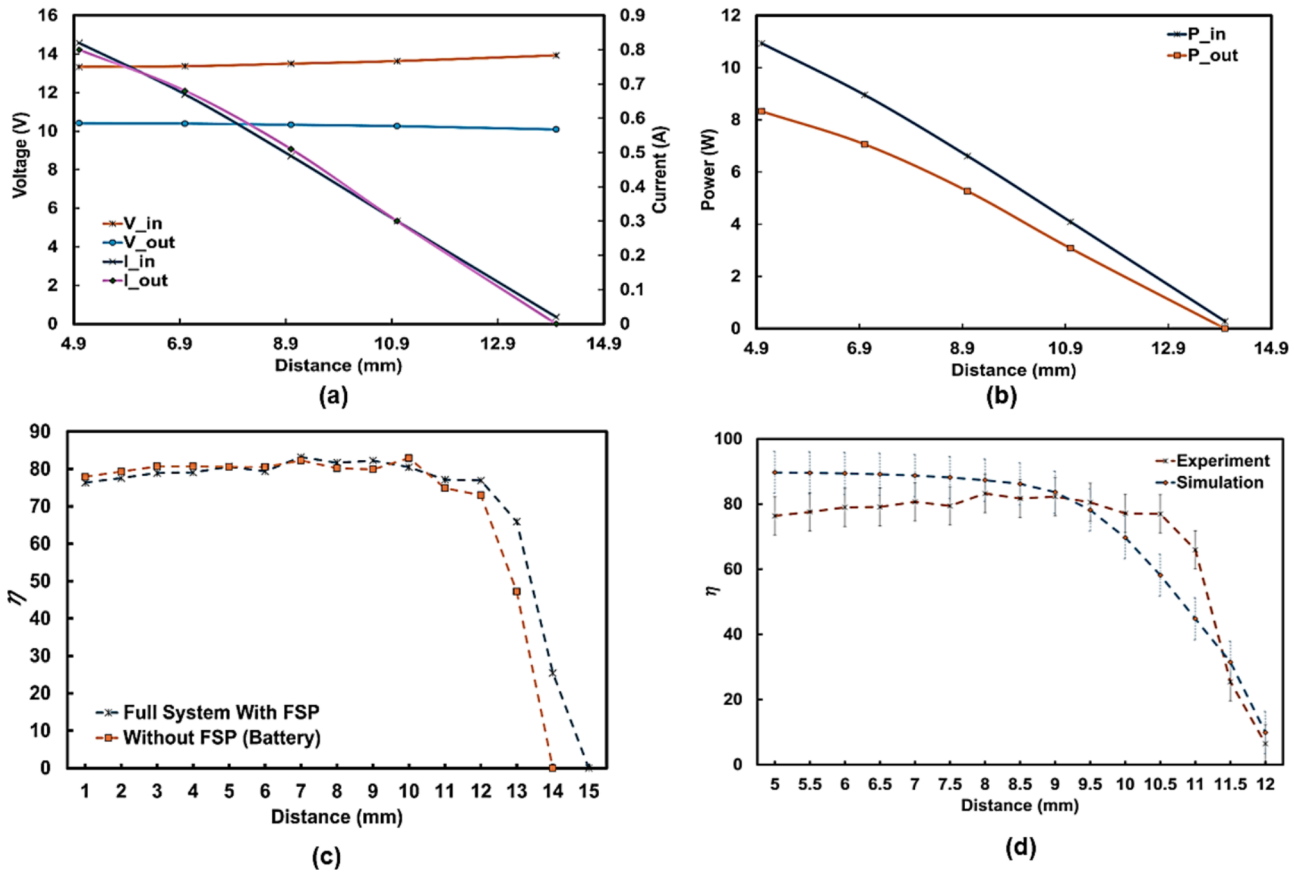


Fig. 11. Experimental WPT performance (a) voltage and current, (b) power transfer, (c) efficiency based on system with and without FS, (d) efficiency based on simulation and experiment.

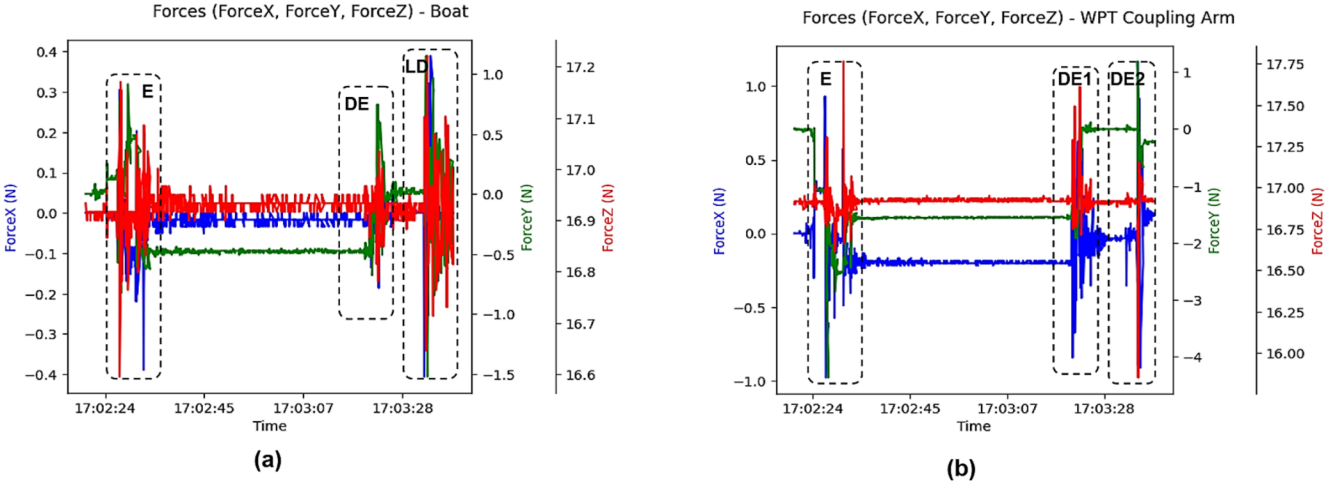


Fig. 12. WPT charging process forces (a) boat, (b) WPT coupling arm.

3.2. Wave tests

The plots in Fig. 13 (a) to (f) shows the analysis of the docking system, focusing on the accelerations, angular velocities, and angular positions for both the boat and the WPT coupling arm. (a) and (b), shows the acceleration experienced by the boat and WPT coupling arm in X, Y, and Z direction during the WPT charging process. For the boat, the phases of WPT engagement (E), disengagement (DE), and boat leaving the dock (LD) are highlighted, reflecting the acceleration experienced by the receiver attached to the boat during these stages. For the WPT coupling arm, the transmitter experiences engagement (E), docking engagement (DE1) where the magnetic coupling transition occur, and arm disengagement (DE2) after charging the boat. These acceleration profiles demonstrate how both the boat and arm respond to external forces, with noticeable spikes during disengagement phases. Figures (c) and (d) illustrate the angular velocities of both the boat and the WPT coupling arm. The boat undergoes changes in angular velocity during engagement, docking engagement, and leaving the dock, while the arm experiences changes during DE1 and DE2. These variations in angular velocity highlight how the system dynamically adjusts its orientation

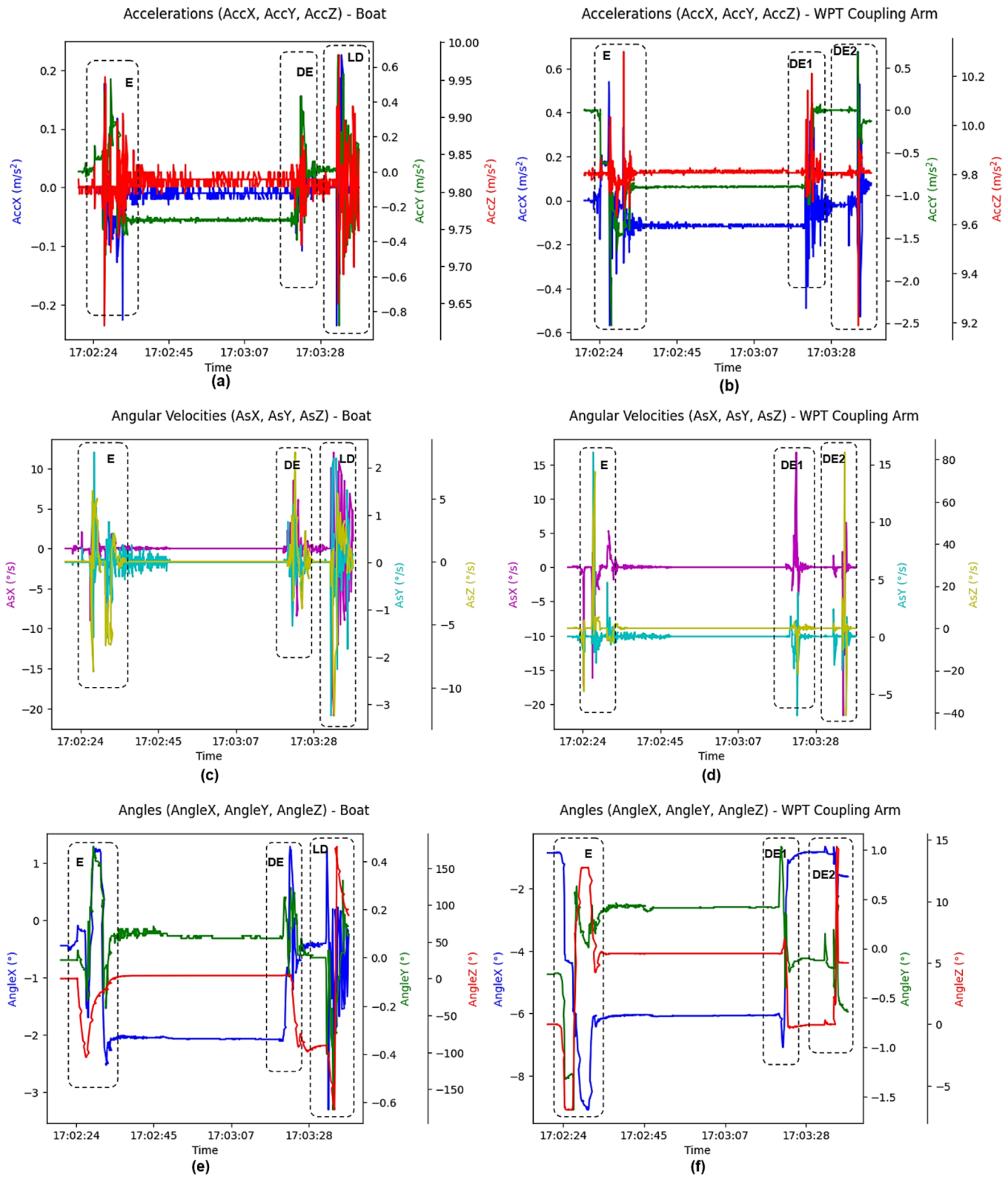


Fig. 13. WPT charging process accelerations, angular velocities, and angular positions for boat, and coupling arm.

during docking and disengagement. Figures (e) and (f) display the angular positions for both components, capturing how the boat and arm adjust their orientation throughout the docking process. These data provide valuable insights into the system's ability to maintain effective wireless power transfer (WPT) coupling during docking operations, ensuring proper alignment despite the external forces acting on the boat and arm during engagement and disengagement due to the robotic movements.

Figs. 14 and 15 show the forces in the X, Y, and Z directions acting on both the boat and the WPT coupling arm under different wave amplitudes (A) from 0.001 m to 0.010 m. Fig. 14(a) and (b) show the forces on the boat and the WPT coupling arm at a wave amplitude of 0.001 m.

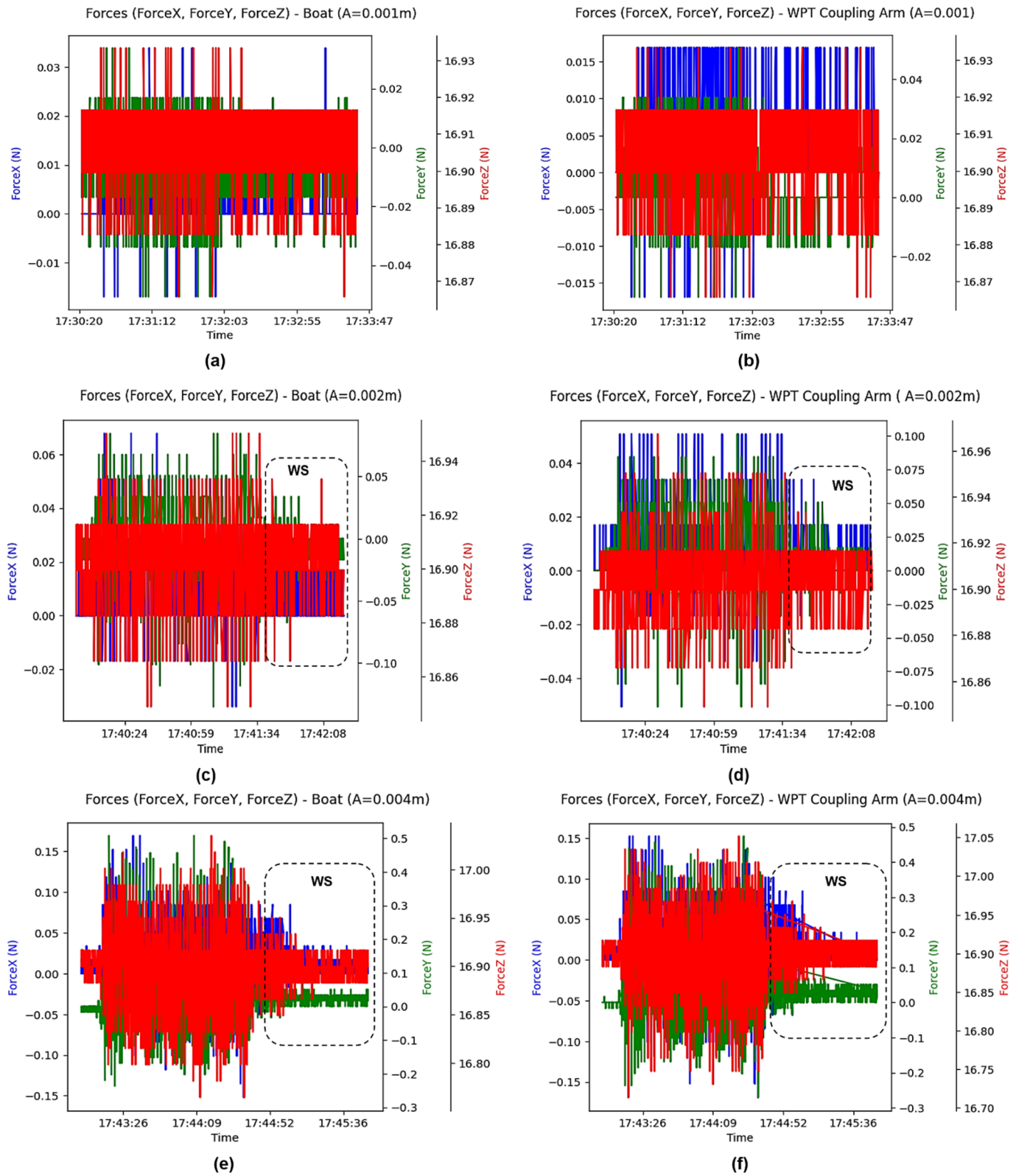


Fig. 14. Forces acting on boat and WPT coupling arm for wave amplitudes of 0.001 m to 0.004 m.

Since the wave amplitude is very small, there is no noticeable wave settling (WS) effect, and the forces remain relatively minimal and stable. The variations in force indicate only minor disturbances due to the small wave amplitude, resulting in limited impact on the boat and coupling arm. Throughout this period, the WPT system continued to charge effectively, with no visible decoupling or misalignment. As the wave amplitude increases to 0.002 m, shown in Fig. 14(c) and (d), the WS effect becomes more apparent, and the forces acting on the boat and coupling arm increase. The time periods corresponding to wave settling are indicated, highlighting the fluctuations in forces during this stage. The increased wave amplitude leads to more pronounced variations in indicating greater interaction between the boat, coupling arm, and the

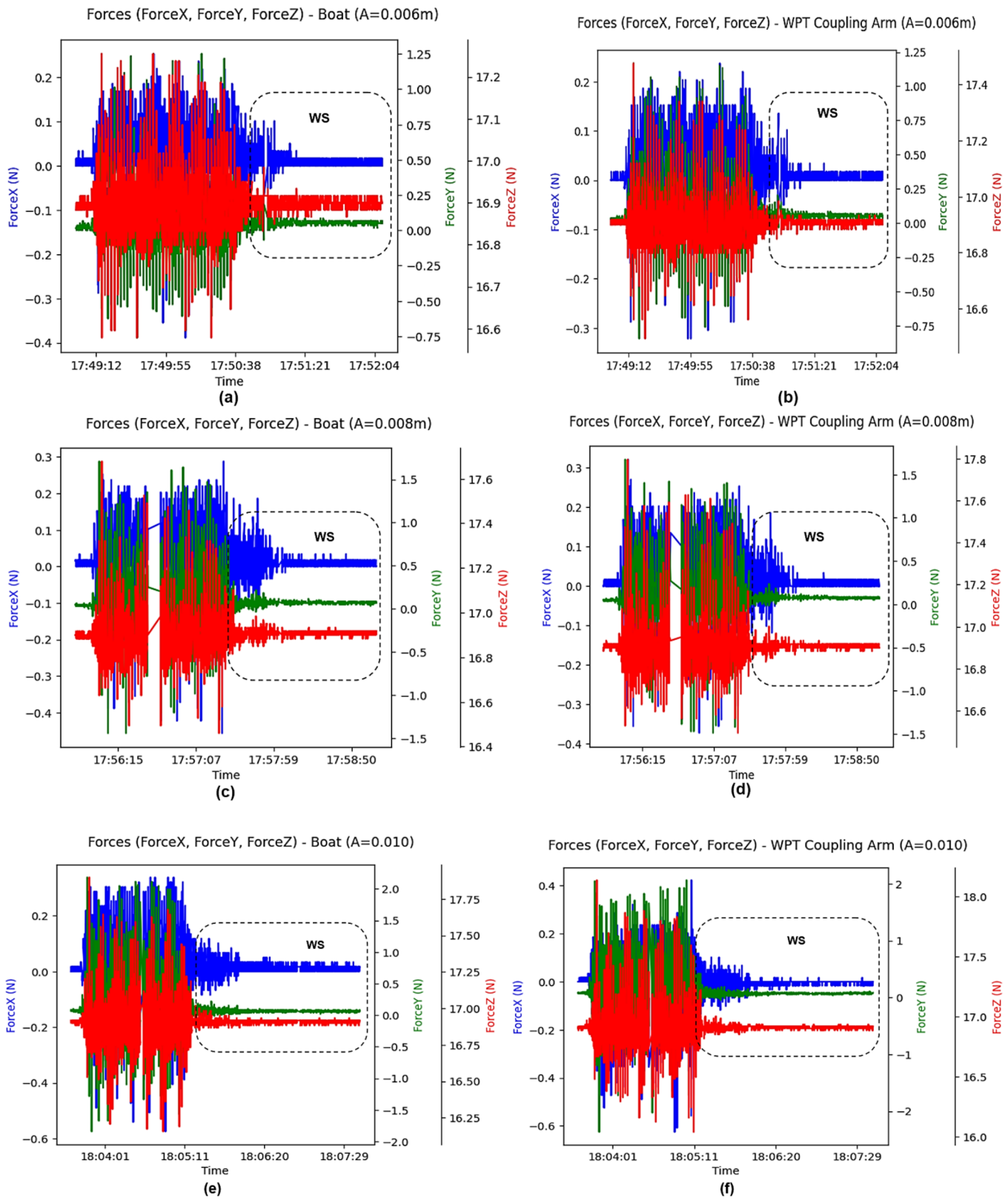


Fig. 15. Forces acting on boat and WPT coupling arm for wave amplitudes of 0.006 m to 0.01 m.

surrounding water due to wave dynamics. Despite these increased forces, the WPT system maintained effective charging with no visible decoupling or misalignment. In Fig. 14(e) and (f), the wave amplitude is further increased to 0.004 m, resulting in even more significant force variations. The WS effect is clearly visible, and the forces acting on both the boat and the WPT coupling arm are higher compared to the lower wave amplitudes. The peaks in forces during the wave settling periods illustrate the increasing impact of larger waves on the stability and alignment of the boat and coupling arm. However, even under these conditions, the WPT system continued to operate effectively, with no

observable decoupling or misalignment. This analysis highlights that as the wave amplitude increases, the forces exerted on the components also rise, necessitating careful consideration of wave dynamics in the design and operation of the docking system to ensure stability during WPT operations, while still maintaining effective charging performance.

Fig. 15 (a) to (f) represent the forces in the X, Y, and Z directions acting on both the boat and the WPT coupling arm under different wave amplitudes. Figures (a) and (b) show the forces on the boat and WPT coupling arm at a wave amplitude of 0.006 m. The wave settling (WS) effect is clearly visible, indicating that the increased wave amplitude has a considerable impact on both the boat and the coupling arm. The forces exhibit noticeable variations, reflecting the dynamic interaction between the boat, coupling arm, and the waves. As the wave amplitude increases to 0.008 m, shown in Figures (c) and (d), the WS effect becomes more pronounced, and the forces acting on the boat and coupling arm increase accordingly. The larger fluctuations in force illustrate that the system is subjected to more significant disturbances, leading to increased interaction between the boat and coupling arm. Despite these forces, the WPT system remains operational without decoupling or misalignment, and effective charging is maintained throughout this phase. In Figures (e) and (f), the wave amplitude is further increased to 0.010 m. At this amplitude, notable separation of approximately 0.005 m was observed. However, based on the experimental efficiency plots in Fig. 11 (c) to (d), the WPT efficiency can be maintained up to 10 mm. The WS effect is clear, and the forces experienced by both the boat and the WPT coupling arm are significant. Despite the observed separation, the WPT system continues to charge effectively, indicating that the coupling mechanism remains functional within the allowable efficiency range. This analysis highlights the robustness of the WPT system under increasing wave amplitudes and separation, demonstrating that the system can sustain efficient power transfer even under challenging conditions, provided the transmitter and receiver separation remains within the 10 mm.

4. Discussion

Shipes electrification and integration of renewable energy sources into WPT systems for maritime application complements the industry's shift toward decarbonisation. By utilizing renewables such as FS with energy storage systems, ports can provide a clean and reliable energy supply for electric and hybrid vessels. This approach not only reduces reliance on carbon-intensive fuels but also aligns with the global push for energy diversification in the maritime sector. The following subsection discusses the scalability, impact and future research direction FSWP for maritime applications.

4.1. Scalability

The use of floating solar technology for maritime applications has several advantages, particularly in contexts where land availability is a concern [21]. The integration of a floating solar power plant with wireless charging technology approach offers a scalable and flexible solution that can be implemented across various port locations. The independent solar plants will not add a capacity burden to the port grid, overcoming the existing capacity limit. However, comprehensive study for of the maritime environment, solar harnessing and energy storage plan is requited which necessitate cost impact assessment and environmental impact analysis. While this study focused on electric yachts, the WPT system's design and results can be scaled to larger vessels such as ferries. Ferries, with larger energy requirements and more substantial wave induced motion, present a unique challenge for WPT systems, but the fundamental principles demonstrated in this paper are applicable. The scaling factor Q is determined by the length ratio between the real yacht and the experimental yacht given in Equation (24). The average length of 14.1 m for the real yacht was reported by [22], providing a realistic baseline for our scaling factor calculations.

$$Scalingfactor Q = \left(\frac{L_{real}}{L_{model}}\right) = \left(\frac{14.1}{0.705}\right) = 20 \tag{24}$$

Where L_{real} is represent real yacht length and L_{model} represent the yacht in this research. The scaling factor Q can also be expressed in terms of the forces acting on the real yacht is given in Equation (25). This scaling shows the significant increase in forces acting on real yacht and emphasises the need for robust structural components. This linear scaling illustrates the increase in forces as vessel mass increases. Docking robotic arms and WPT receivers must be designed to manage these significant forces. Meanwhile, wave heights encountered by vessels can also be scaled by Equation (26).

$$F_{real} = F_{model} \times Q^2 \tag{25}$$

$$A_{realwave} = Q \times A_{realwave} \tag{26}$$

As wave amplitude (A) increases, forces due to waves also increase. Advanced stabilization mechanisms would be required to maintain proper alignment during docking in open sea conditions. Scaling the WPT system from the experimental 50 W system to larger system involves several system adjusting based on power demands, efficiency and transfer distance. Real yacht requires more power, and the separation between transmitter and receiver will also increase. To determine the required battery capacity for real yacht, we analyse the relationship between the battery capacities of the model yacht and a typical full-sized yacht based on Equation (27). The model yacht uses a 2000 mAh battery, and based on industry standards, a larger yacht may require a capacity of around 500Ah to meet operational needs.

$$\lambda_{realpower} = \lambda_{modelpower} \times Q^{\alpha} \tag{27}$$

$$500Ah = 2Ah \times 20^{\alpha}$$

$$\alpha = \left(\frac{log(250)}{log(20)}\right) = \left(\frac{2.3979}{1.3010}\right) = 1.84$$

Where $\lambda_{modelpower}$ and $\lambda_{realpower}$ represent the battery capacity of model yacht and real yacht respectively. The scaling exponent α is determined to be 1.84, indicating that for real yacht, the required battery capacity grows significantly, reflecting the increased energy demands of larger vessels. This scaling approach can help in designing WPT systems for larger maritime applications, ensuring they meet energy needs effectively. The same approach can be adopted for other vessel and ferries. However, it's important to note as vessel or ferry size increases, power demands increase, making the FSWPT system design optimisation more crucial to scale it up. WPT systems for larger vessels may require enhanced efficient measures, such as optimised coil designs to ensure efficient energy transfer. Three basic design adjustments are necessary as follows to scale the experimental results for larger vessels.

- **Structural Reinforcement**: Docking arms and WPT receivers must be structurally reinforced to manage the increased forces due to vessel length and mass.
- **Advanced Stabilization Systems**: Docking systems will require active stabilization to manage larger wave amplitudes and maintain proper WPT coupling in challenging conditions.
- **Power Optimization**: Larger vessels, require significantly higher power outputs, and WPT systems must be optimised to minimize power losses during transfer over greater distances.

4.2. Impacts and future work

The integration of WPT with FS, into port infrastructure represents a significant step forward in the electrification of maritime operations. This research emphasizes the potential of WPT technology in reducing emissions, enhancing energy efficiency, and supporting the global transition to sustainable energy systems. The FSWPS maximise the

utilisation of water surfaces for solar energy harvesting and eliminates the need for land area or disruptive activity on ports. The WPT eliminates the need for expensive underwater cabling, although FS practical implementation faces significant challenges as reported in the following research [23–26]. The efficiency of WPT systems remains a critical limitation as reported in [27], as energy transmission losses increase with distance due to marine environment factors, potentially undermining the economic and environmental benefits of the system. Moreover, while FS offers advantages such as reduced water evaporation and minimal land use, the environmental impact of introducing electromagnetic fields into aquatic ecosystems is not yet fully understood and could have unforeseen consequences on marine biodiversity [28]. Additionally, the high initial costs and technological complexities of integrating FS [29], and WPT raise questions about its scalability and accessibility, especially in low-resource settings. This could be an area for further study. Despite these challenges, FSWPT represents a cutting-edge approach that could redefine renewable energy deployment, but its success depends on addressing these technological, economic, and environmental issues through rigorous research and innovation. Our work has demonstrated FSWPT feasibility through controlled wave tank experiments. The experiments simulated dynamic port conditions, including docking, charging, and departure, highlighting alignment sensitivity as a critical factor for achieving optimal energy transfer efficiency. Misalignments can lead to significant energy losses, making the development of advanced alignment mechanisms or self-correcting systems a priority for future research. The findings also underline the importance of modular and scalable FSWPT designs, which allow ports to adapt the technology to varying energy demands.

The advantages of FSWPT align with broader trends in the maritime and shipping industries, which are undergoing a significant technological transition toward decarbonization [30]. The increasing adoption of carbon–neutral fuels, battery energy storage systems (BESS), and hybrid propulsion technologies reflects this shift [31]. Notably, the trend of ordering vessels with alternative fuel propulsion systems and integrating renewable energy sources into ship operations is accelerating. For short-range vessels, in particular, battery/hybrid propulsion is becoming increasingly prevalent, offering a practical pathway to achieving the industry's decarbonization goals. Research on hybrid propulsion systems and BESS highlights their versatility and application across various maritime scenarios. In [32], BESS systems are used for peak shaving, load levelling, spinning reserve, and load response, providing operational flexibility and efficiency. These systems are particularly valuable for short-range vessels, where the energy requirements align well with the capabilities of battery-driven propulsion. Furthermore, recent advancements by leading maritime manufacturers in hybrid and electric propulsion systems demonstrate the rapid progress and market adoption of these technologies as way to decarbonisation [33,34]. Integrating WPT systems into this evolving landscape offers a seamless, contactless solution for charging electric and hybrid vessels, further enhancing their operational efficiency and environmental benefits.

Economic analyses of the viability of integrating WPT systems into port operations with FS need to be investigated. Research by [31] reported that renewable energy that incorporate muti-energy system exceeds 72 % in terms of economic and environmental metrics compare to grid sources, and the Levelized Cost of Energy (LCOE) is competitive with traditional energy sources. These findings align with studies on renewable energy systems in shipyards, where hybrid configurations with solar PV, wind turbines, and diesel generators demonstrated short payback periods and significant economic benefits [35]. Such insights underscore the importance of optimizing system configurations to maximize both environmental and economic performance. However, several challenges remain, including the need to address technical difficulties in marine environments, mitigate environmental impacts on aquatic ecosystems, and navigate regulatory complexities. These challenges are consistent with those faced in the broader adoption of renewable and hybrid energy systems in the shipping industry. The environmental assessments and streamlined regulatory frameworks are critical to ensuring the successful deployment of FSWPT systems while protecting marine ecosystems. We have demonstrated the feasibility of FSWPT for electric vessel charging by performing a docking, charging, and departure in a wave tank. Simulations and physical testing are used to verify this concept, where the main findings were sensitivity to alignment, which is very crucial in reaching the ultimate efficiency. However, more work is needed to scale up the system. Table 3 present a summary of a vantages, considerations, and future research directions of FSWPT for maritime applications can be summarised as follows.

a) Future research can focus on modular FSWPT design optimization to cater to a range of vessel sizes, ensuring flexibility in integration with different fleet configurations. Explore modular battery storage systems to enable greater energy independence for vessels, ensuring consistent power supply during times of low solar exposure. Improve energy storage integration with the FSWPT system to maintain reliable off-grid operation when vessels are away from charging stations or shore-based power. Develop modular energy management systems that allow flexible deployment on large fleets of electric ferries, cargo ships, and luxury vessels. Explore how modular off-grid systems can scale with vessel size, enabling fleets to operate autonomously and reduce reliance on traditional, centralized charging stations. In addition, the switching frequency is an important factor, future research can investigate its impact on system efficiency and power transfer.
b) Investigate deployment of off-grid modular systems to support remote maritime operations and isolated areas with limited infrastructure. Focus on island communities, oceanic research stations, and offshore operations. Provide self-sustaining energy solutions for

Table 3
Advantages considerations, and challenges of FSWPT for maritime applications.

Category	Advantages
Land Conservation	• Utilizes water surface, conserving valuable land space for agriculture, housing, or other uses. The WPT can be standalone independent of the grid.
Increased Efficiency	• Water bodies cool the solar panels, enhancing their efficiency compared to land-based installations. • WPT less unaffected hostile environments.
Reduced Evaporation	• FS helps conserve water in reservoirs, particularly in regions facing water scarcity.
Less Competition for Resources	• Non-invasive; floating solar has less impact on land ecosystems and does not require land clearing.
Hybrid Systems Potential	• Can coexist with aquaculture, allowing for dual use of water bodies and improving the economic viability of both ventures. • Can be integrated with other renewable energy system such as wind, wave energy harvesters.
Infrastructure Resilience	• Easy, convenient, safe, and reliable to use due to elimination of direct electrical contact with cable connection. • Less susceptible to damage from floods or extreme weather conditions compared to ground-mounted solar systems.
Modular and Scalable	• Designed in modular units, making it easier to scale up or down based on energy needs.
Considerations and Challenges	
Installation and Maintenance	• Technical challenges in anchoring panels securely and ensuring operational integrity in marine conditions.
Environmental Impact	• Potential disruption to aquatic ecosystems and local wildlife, depending on the location of installation.
Weather and Marine Conditions	• Must withstand harsh marine environments, including high winds, waves, and saltwater corrosion.
Regulatory and Permitting Issues	• Navigating the regulatory landscape for maritime installations can be complex and may require multiple permits.
Connectivity to Grid	• Connecting floating solar to existing electrical grids may require additional infrastructure, especially if installed far from shore.

vessels and maritime facilities in areas where grid-based power is not available.

c) Develop hybrid off-grid energy systems that combine solar power with other renewable sources such as wind and wave energy, creating a resilient energy network for vessels. Ensure continuous energy availability in harsh conditions by integrating multiple renewable technologies, such as offshore wind or wave energy harvesters.
d) Deploy modular WPT systems to create off-grid charging stations in remote docking locations, providing charging infrastructure where shore-based power is unavailable. Explore energy management strategies to ensure cost-effective and environmentally friendly WPT systems capable of delivering reliable power for remote maritime vessels.
e) Investigate autonomous vessels that operate in off-grid conditions, integrating FSWPT systems with advanced power management to allow self-sustaining operation without human oversight. Focus on the ability of autonomous vessels to self-charge using floating solar power and WPT systems, eliminating the need for human-operated refuelling stations.
f) Regulatory Framework and Policy Development – Develop streamlined permitting processes and regulations that promote the safe deployment of floating solar WPT systems while balancing the protection of marine ecosystems and promoting green technology. Establish standards and guidelines to regulate the integration of floating solar systems with WPT, ensuring compliance with safety, environmental, and operational protocols in maritime environments.
g) Conduct economic viability studies to determine the cost-effectiveness of the FSWPT system compared to traditional land-based energy sources, focusing on long-term sustainability and financial feasibility. Investigate return on investment (ROI) for vessels using off-grid WPT systems, evaluating the economic benefits from fuel savings, maintenance costs, and reduced infrastructure dependency.

5. Conclusions

Motivated by the goal of maritime decarbonisation, ship charging stations powered by clean renewable energies are urgently required. Meanwhile, the potential of WPT in maritime environments could be particularly valuable as removing the human labour and cables on side, increasing efficiency and minimizing risks. In addition, independent renewable energy charging stations are desirable as merging into existing grid poses a challange to the maximum capacity. This study successfully designed, simulated, and experimentally tested a floating solar wireless power transfer system for electric yachts, incorporating an innovative docking mechanism with an automatic gate and robotic arm for precise alignment. The off-grid modularity of the floating solar wireless power transfer system enables scalable, flexible, and sustainable energy delivery for maritime applications, ensuring energy independence for vessels in remote locations without reliance on shore-based power, while also reducing strain on the grid by generating and supplying renewable energy directly to ships without adding additional load to existing electrical infrastructure. The WPT system achieved high power transfer efficiency of 82 % under both simulated and experimentally conditions, demonstrating its potential to provide contactless, automated charging in dynamic maritime environments. Experimental results demonstrated significant force variations during WPT phases with maximum forces of 1.5 N, 1.5 N, and 1.4 N along *XYZ* on the boat, while a maximum force of 2 N, 5 N and 1 N along *XYZ* on the WPT coupling arm, respectively. The maximum acceleration and angle orientation are obtained to be 0.4 m/s^2 with angles of 3° along *X* direction on the boat showing effective stabilisation of forces throughout the WPT. A complete video of the docking, coupling and charging process can be found in the supplementary material. While the system exhibited sensitivity to misalignment, the robotic arm's real-time adjustments helped maintain efficiency even in the presence of induced wave motion. The scalability of the system to real yacht size has been discussed, suggesting that with proper adjustments, the technology could be adapted to meet the energy demands of large-scale maritime applications. A scaling factor of 20 was obtained which translates to a real wave conditions of 0.2 m, and a scaling exponent for power was estimated to be 1.8. Mechanical and sustainable advantages of the novel systems were discussed. Future work should focus on optimising the system for larger vessels, testing in real-port conditions, and studying the economic and carbon-reduction performance. This research lays the groundwork for the broader adoption of FS and WPT technologies in the maritime sector, supporting the shift towards cleaner and more efficient energy solutions.

CRediT authorship contribution statement

Khalifa Aliyu Ibrahim: Writing – original draft, Visualization, Validation, Software, Methodology, Formal analysis, Data curation. **Timothé Le Maréchal:** Visualization, Validation, Software, Methodology, Formal analysis, Data curation. **Patrick Luk:** Supervision, Resources, Methodology, Investigation, Funding acquisition, Conceptualization. **Qing Qin:** Writing – review & editing, Writing – original draft, Investigation. **Luofeng Huang:** Writing – review & editing, Supervision, Resources, Project administration, Methodology, Investigation, Funding acquisition, Conceptualization. **Ying Xie:** Supervision, Resources, Investigation, Funding acquisition. **Patrick Verdin:** Supervision, Resources, Investigation, Funding acquisition. **Zhenhua Luo:** Supervision, Resources, Methodology, Investigation, Funding acquisition, Conceptualization.

Declaration of competing interest

The authors declare that they have no known competing financial interests or personal relationships that could have appeared to influence the work reported in this paper.

Acknowledgements

This work is part of a project that has received funding Transport Research and Innovation Grants supported by UK Department for Transport and Connected Places Catapult under Grant Agreement No. TRIG2023-30066 - Design of a floating solar charge station for the electric vessels at the Port of Dover.

Appendix A. Supplementary data

Supplementary data to this article can be found online at https://doi.org/10.1016/j.enconman.2025.119738.

Data availability

All data underlying the results are available as part of the article and no additional source data are required.

References

[1] Prados JMM. The decarbonisation of the maritime sector: Horizon 2050. Brodogradnja 2024;75:1–26. https://doi.org/10.21278/brod75202.
[2] Ning Y, Wang L, Yu X, Li J. Recent development in the decarbonization of marine and offshore engineering systems. Ocean Eng 2023;280:114883. https://doi.org/10.1016/j.oceaneng.2023.114883.
[3] Frković L, Ćosić B, Falkoni A, Pukšec T, Vladimir N. Shore-to-ship: Enabling the electrification sustainability of maritime transport with the nexus between berthed cruise ships and renewables in the isolated energy systems. Ocean Eng 2024;302:117537. https://doi.org/10.1016/j.oceaneng.2024.117537.
[4] Agarwala P, Chhabra S, Agarwala N. Using digitalisation to achieve decarbonisation in the shipping industry. J Int Maritime Safety, Environ Affairs, Shipping 2021;5:161–74. https://doi.org/10.1080/25725084.2021.2009420.

[5] von Malmborg F. Advocacy coalitions and policy change for decarbonisation of international maritime transport: The case of FuelEU maritime. Marit Transport Res 2023;4:100091. https://doi.org/10.1016/j.martra.2023.100091.
[6] Choi C-K, Iam I-W, Hoi I-U, Lam C-S. An Inductive Power Transfer Converter with Irradiance-Adaptive Hybrid MPPT Control Strategy for Floating-PV System. In: in: IECON 2021–47th Annual Conference of the IEEE Industrial Electronics Society. IEEE; 2021. p. 1–6. https://doi.org/10.1109/IECON48115.2021.9589492.
[7] Liu J, Yu F, He B, Soares CG. A review of underwater docking and charging technology for autonomous vehicles. Ocean Eng 2024;297:117154. https://doi.org/10.1016/j.oceaneng.2024.117154.
[8] Lin M, Lin R, Yang C, Li D, Zhang Z, Zhao Y, et al. Docking to an underwater suspended charging station: Systematic design and experimental tests. Ocean Eng 2022;249:110766. https://doi.org/10.1016/j.oceaneng.2022.110766.
[9] Huang L, Yang Y, Khojasteh D, Ou B, Luo Z. Floating solar power loss due to motions induced by ocean waves: An experimental study. Ocean Eng 2024;312:118988. https://doi.org/10.1016/j.oceaneng.2024.118988.
[10] Karimi S, Zadeh M, Suul JA. Shore Charging for Plug-In Battery-Powered Ships: Power System Architecture, infrastructure, and Control. IEEE Electrif Mag 2020;8:47–61. https://doi.org/10.1109/MELE.2020.3005699.
[11] Mahdi H, Hoff B, Ostrem T. A Review of Power Converters for Ships Electrification. IEEE Trans Power Electron 2023;38:4680–97. https://doi.org/10.1109/TPEL.2022.3227398.
[12] Rong E, Sun P, Yang G, Xia J, Liu Z, Li S. 5-kW, 96.5% Efficiency Capacitive Power Transfer System With a Five-Plate Coupler: Design and Optimization. IEEE Trans Power Electron 2025;40:2542–55. https://doi.org/10.1109/TPEL.2024.3462410.
[13] Zhang C, Dai J, Ang KK, Lim HV. Development of compliant modular floating photovoltaic farm for coastal conditions. Renew Sustain Energy Rev 2024;190:114084. https://doi.org/10.1016/j.rser.2023.114084.
[14] Song Z-Y, Chhetri P, Ye G, Lee P-T-W. Green maritime logistics coalition by green shipping corridors: a new paradigm for the decarbonisation of the maritime industry. Int J Log Res Appl 2023;1–17. https://doi.org/10.1080/13675567.2023.2256243.
[15] Shyam B, Kanakasabapathy P. Feasibility of floating solar PV integrated pumped storage system for a grid-connected microgrid under static time of day tariff environment: A case study from India. Renew Energy 2022;192:200–15. https://doi.org/10.1016/j.renene.2022.04.031.
[16] Hooper T, Armstrong A, Vlaswinkel B. Environmental impacts and benefits of marine floating solar. Sol Energy 2021;219:11–4. https://doi.org/10.1016/j.solener.2020.10.010.
[17] Khojasteh D, Shamsipour A, Huang L, Tavakoli S, Haghani M, Flocard F, et al. A large-scale review of wave and tidal energy research over the last 20 years. Ocean Eng 2023;282:114995. https://doi.org/10.1016/j.oceaneng.2023.114995.
[18] Kavitha M, Bobba PB, Prasad D. Comprehensive mathematical modelling and experimental analysis of a wireless power transfer system for neighborhood electric vehicles. In: in: 2015 IEEE International WIE Conference on Electrical and Computer Engineering (WIECON-ECE). IEEE; 2015. p. 275–9. https://doi.org/10.1109/WIECON-ECE.2015.7443916.
[19] Jadhav K, Urlam V, Harer R, Naik S, Deshpande A, Jadhav H. Design and Implementation of Resonance based Wireless Power Transfer System. In: in: 2020 IEEE International Conference for Innovation in Technology (INOCON). IEEE; 2020. p. 1–5. https://doi.org/10.1109/INOCON50539.2020.9298414.
[20] Yang Y, Mi C, Ou B, Wong A, Duffy JG, Wood T, et al. A comparative experimental study on the hydrodynamic performance of two floating solar structures with a breakwater in waves. Sol Energy 2024;284:113029. https://doi.org/10.1016/j.solener.2024.113029.
[21] Shi W, Yan C, Ren Z, Yuan Z, Liu Y, Zheng S, et al. Review on the development of marine floating photovoltaic systems. Ocean Eng 2023;286:115560. https://doi.org/10.1016/j.oceaneng.2023.115560.
[22] Marco Ugolini G, Ivaldi E. Tourist Ports and Yachting: The Case of Sardinia. Revista de Estudios Andaluces 2017:429–52. https://doi.org/10.12795/rea.2017.i34.15.
[23] Bai B, Xiong S, Ma X, Liao X. Assessment of floating solar photovoltaic potential in China. Renew Energy 2024;220:119572. https://doi.org/10.1016/j.renene.2023.119572.
[24] Ramanan CJ, Lim KH, Kurnia JC, Roy S, Bora BJ, Medhi BJ. Design study on the parameters influencing the performance of floating solar PV. Renew Energy 2024;223:120064. https://doi.org/10.1016/j.renene.2024.120064.
[25] Delacroix S, Bourdier S, Soulard T, Elzaabalawy H, Vasilenko P. Experimental modelling of a floating solar power plant array under wave forcing. Energies (Basel) 2023;16:5198. https://doi.org/10.3390/en16135198.
[26] Rashid FL, Al-Obaidi MA, Hussein AK, Akkurt N, Ali B, Younis O. Floating solar stills and floating solar-driven membranes: Recent advances and overview of designs, performance and modern combinations. Sol Energy 2022;247:355–72. https://doi.org/10.1016/j.solener.2022.10.044.
[27] Lin R, Lin M, Yang C, Li D, Zhang Z. Frequency optimization of the AUV wireless charging system for minimum energy dissipation. Ocean Eng 2024;312:119066. https://doi.org/10.1016/j.oceaneng.2024.119066.
[28] Wang Y, Wright LA. A comparative review of alternative fuels for the maritime sector: economic, technology, and policy challenges for clean energy implementation. WORLD 2021;2:456–81. https://doi.org/10.3390/world2040029.
[29] Vakili S, Schönborn A, Ölçer AI. Techno-economic feasibility of photovoltaic, wind and hybrid electrification systems for stand-alone and grid-connected shipyard electrification in Italy. J Clean Prod 2022;366:132945. https://doi.org/10.1016/j.jclepro.2022.132945.
[30] Nisiforou O, Shakou LM, Magou A, Charalambides AG. A roadmap towards the decarbonization of shipping: A participatory approach in Cyprus. Sustainability 2022;14:2185. https://doi.org/10.3390/su14042185.
[31] Tang D, Chen Z, Zhao W, Yuan Y, Yuan C, Guerrero JM, et al. Sustainable mega-seaports with integrated multi-energy systems: Life-cycle environmental and economic evaluation. J Clean Prod 2024;143905. https://doi.org/10.1016/j.jclepro.2024.143905.
[32] Kolodziejski M, Michalska-Pozoga I. Battery Energy Storage Systems in Ships' Hybrid/Electric Propulsion Systems. Energies (Basel) 2023;16:1122. https://doi.org/10.3390/en16031122.
[33] Bach H, Hansen T. IMO off course for decarbonisation of shipping? Three challenges for stricter policy. Mar Policy 2023;147:105379. https://doi.org/10.1016/j.marpol.2022.105379.
[34] Barreiro J, Zaragoza S, Diaz-Casas V. Review of ship energy efficiency. Ocean Eng 2022;257:111594. https://doi.org/10.1016/j.oceaneng.2022.111594.
[35] Ghosh A. A comprehensive review of water based PV: Flotavoltaics, under water, offshore & canal top. Ocean Eng 2023;281:115044. https://doi.org/10.1016/j.oceaneng.2023.115044.

DSPACE

https://dspace.org/

Floating solar wireless power transfer system for electric ships: design and laboratory tests

Ibrahim, Khalifa Aliyu; Maréchal, Timothé Le; Luk, Patrick Chi-Kwong; Qin, Qing; Huang, Luofeng ...

2025-05-15
Elsevier
https://doi.org/10.1016/j.enconman.2025.119738
Ibrahim KA, Maréchal TL, Luk P, et al., (2025) Floating solar wireless power transfer system for electric ships: design and laboratory tests. Energy Conversion and Management, Volume 332, May 2025, Article number 119738

Downloaded from a DSpace repository. https://dspace.org/